

6
7
8
9
10
11

A European endeavor for optimizing Zonal Isolation, Drilling and Exploitation of EGS projects

12
13
14

THE ST2 BOREHOLE IN THE BEDRETTO UNDERGROUND LAB FOR GEOSCIENCES AND GEOENERGIES (BULGG):

15
16

ACTIVITIES CARRIED OUT IN THE FRAMEWORK OF THE
GEOthermica/ZoDrEx RESEARCH PROJECT

17
18

Authors: R. Castilla, P. Meier, F. Bethmann, F. Christie and F. Serbeto.

19
20

Geo-Energie Suisse

21
22
23

Date: December 2021



The GEOthermica is supported by the European Union's HORIZON 2020 programme for research, technological development and demonstration under grant agreement No 731117

25 Contents

26	1. Introduction	Error! Bookmark not defined.
27	2. Conventions used in this report.....	4
28	3. Characterization of the ST2 borehole	4
29	3.1 Borehole geometry and post-drilling condition.....	4
30	3.2 Lithology.....	11
31	3.3 Structure	13
32	3.4 Fluids.....	15
33	4. Summary of activities in the framework of ZoDrEx	16
34	5. Hydrotests.....	21
35	6. Notching.....	23
36	6.1 October 2020	24
37	6.2 March 2021	26
38	6.3 May 2021	27
39	6.4 July-October 2021	27
40	7. Minifrac – October 2020	32
41	8. Stimulations	37
42	8.1 November 2020	39
43	8.1.1 Intervals.....	39
44	8.1.2 Fluid Temperature & Conductivity.....	41
45	8.1.3 Newly formed Breakouts	42
46	8.1.4 Shear displacement on pre-existing fractures	44
47	8.1.5 Influence of notching on stimulation results	48
48	8.2 May 2021	50
49	8.2.1 Intervals.....	50
50	8.3 October 2021	50
51	8.3.1 Intervals.....	50
52	9. References	51
53	10. Annexes.....	52
54	10.1 Stimulation November 2020 – Full borehole logs	53
55		

56 1. Executive Summary

57 The present report aims to describe the ST2 borehole, and the successive activities carried out in the
58 framework of the GEOTHERMICA/ZoDrEx research project. The content of the report is relevant to
59 the work packages 2.1 (Characterization of the boreholes through logging and hydro-testing), 3.4
60 (Stimulation of various segments with different zonal isolation means) and 3.5 (Analysis of the data
61 collected in WP 3.4 using analytical and advanced numerical models).

62 ST2 was drilled in July 2020 and it is part of an array of boreholes in the BULGG aiming to test
63 methodologies and workflows to improve the development of geo energy projects in granitic rocks.
64 Ten other long boreholes (100m to 400m) have been drilled in the vicinity of ST2 for monitoring or
65 injecting purposes. ST2 is the second longest borehole of the array with a total length of 350m.
66 Details on the position and geometry of ST2 are given in chapter 3.1 Borehole geometry and post-
67 drilling condition.

68 The BULGG is located inside a granitic intrusion (The Rotondo granite) in the Gotthard massif in the
69 Swiss Alps. Some general and specific geological considerations are described in this report (3
70 Characterization of the ST2 borehole) and a detailed structural analysis covering the whole BULGG is
71 available in the report "Structural characterization of the Bedretto Underground Laboratory for
72 Geoennergies (BULGG)".

73 A general overview of the activities carried out in ST2 is given in chapter 4 Summary of activities in
74 the framework of ZoDrEx, indicating their chronological order as well as their respective depths.
75 Carried out activities include hydrotests (chapter 5), notching (chapter 6), minifrac tests (chapter 7)
76 and shear stimulations (chapter 8). The works carried out cover the bottom-most 100m of the
77 borehole between depths 150m and 350m but the majority of activities were concentrated in the
78 deeper 50m (300-350m).

79 Extensive logging was carried out before and after each one of the above listed activities. Logs
80 acquired in a repetitive way at different stages of the project include spectral gamma ray, image logs
81 (acoustic and optical televiwers) and fluid temperature and conductivity. Other logs acquired in a
82 one-time basis are borehole GPR and full wave sonic. A campaign of flowmeter measurements was
83 unsuccessful to define the flow rate in the borehole as well as the feeding zones from the formation
84 and for that reason the results are not included here.

85 Examination of the logs before and after minifrac tests didn't reveal any significant effect on the
86 borehole walls. The presence of natural fractures, observed mainly in the optical televiwer might
87 explain the lack of new tensile fracturing associated to these tests.

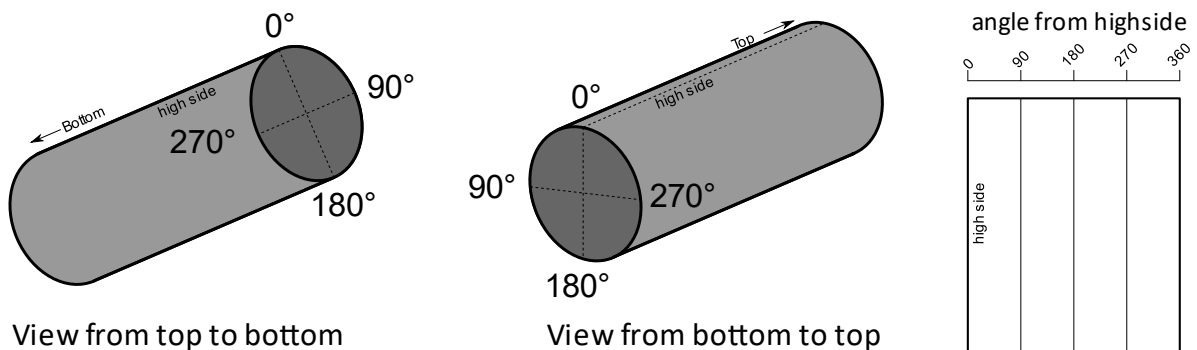
88 Analyses of the acoustic televiwer logs revealed that the stimulation treatment carried out during
89 November 2020 triggered shear displacement in at least 3 structures belonging to 3 different
90 intervals (intervals 1, 2 and 5). This displacement is in the order of 2-5 mm and it is associated to
91 deformation extending 20-50 cm away from the fractures. Details of this analysis can be found in
92 chapter 8.1.4 Shear displacement on pre-existing fractures.

93 The evidence on the effectiveness of notching treatments to increase the probability of cross-
94 borehole fractures is not conclusive. The almost omnipresent natural fractures and their response to
95 injection might have masked the benefits expected from notching.

96 **2. Conventions used in this report.**

97 The official name of the Bedretto lab is the Bedretto Underground Lab for Geosciences and
 98 Geoennergies (BULGG). Bedretto lab and BULGG are used in this report interchangeably.

99 All depths in boreholes correspond to measured depth in meters unless stated otherwise. Image logs
 100 are loaded and interpreted in a "high side" reference system. This was necessary as ST2 is an inclined
 101 borehole and the reference to the North makes no sense. A High-side reference means that the
 102 horizontal axis in the logs represents the angle from the highest line in the borehole. This angle
 103 increases clockwise when looking towards the bottom of the borehole (Figure 1). The left, vertical
 104 axis of the log represents angle zero (aka. the high side).



105

106 *Figure 1. The "High side" of the borehole is the reference used in image logs from deviated wells.*
 107 *When unravelling the image log to display it in 2D, the high side (0°) coincides with the left border of*
 108 *the log. The angle increases clockwise when looking down the borehole.*

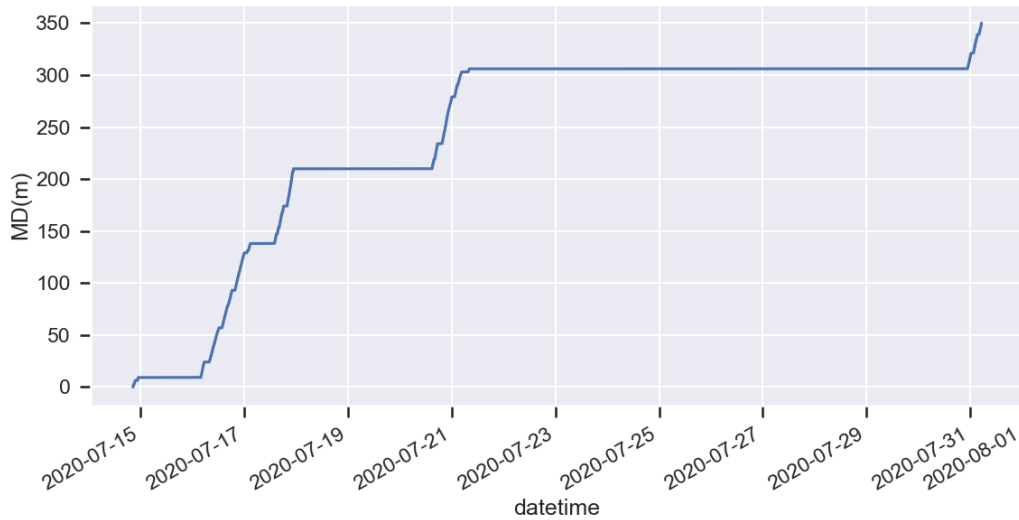
109 Borehole orientations are given as azimuth (clockwise angle from north, 0°-360°) and inclination
 110 (angle from a vertical axis that is pointing down, 0°-90°). An inclination of 0° corresponds to a vertical
 111 borehole while 90° describes a horizontal borehole.

112 The orientation of planar elements (i.e faults & fractures) is given in strike (clockwise azimuth from
 113 north of a horizontal line in the plane) and dip (angle from the horizontal of a line perpendicular to
 114 the strike). A plane given as N50°/70° is oriented NE-SW and dips to the SE. A plane given as
 115 N230°/70° will also be oriented NE-SW but dips towards the NW.

116 **3. Characterization of the ST2 borehole**

117 **3.1 Borehole geometry and post-drilling condition**

118 ST2 was spudded on July 14th, 2020, and was completed on the 31st of July. It took approximately 6
 119 days to drill the first 300m. A pause of 10 days in the drilling operations delayed the completion of
 120 the borehole. The final 50 m were drilled on July 31st (Figure 2).

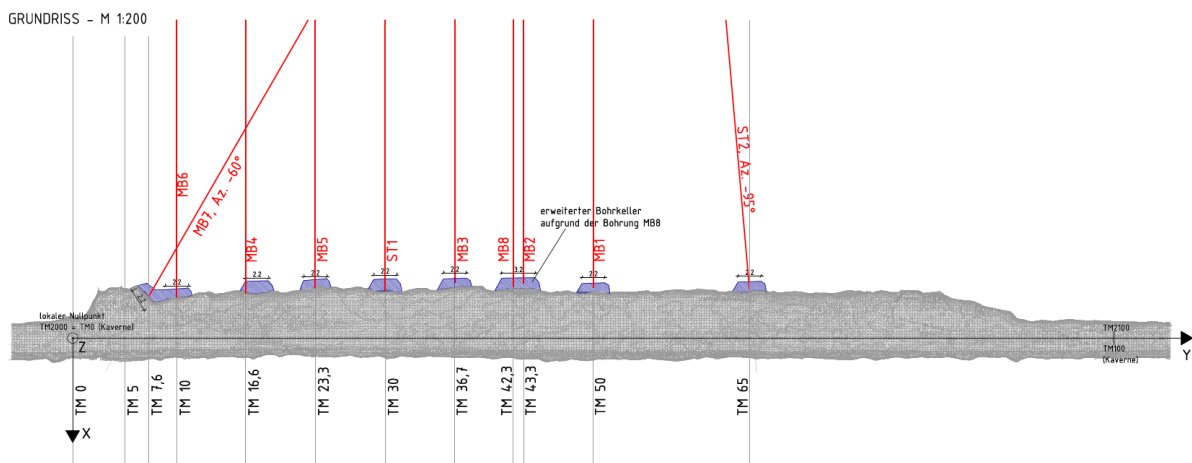


121

122

Figure 2 Drilling progress of ST2.

123 ST2's wellhead lies at tunnel coordinate (TM) 2065m. This is 15m NW of the MB1 wellhead. ST2 is
 124 the northernmost borehole in the Bedretto lab (Figure 3).



125

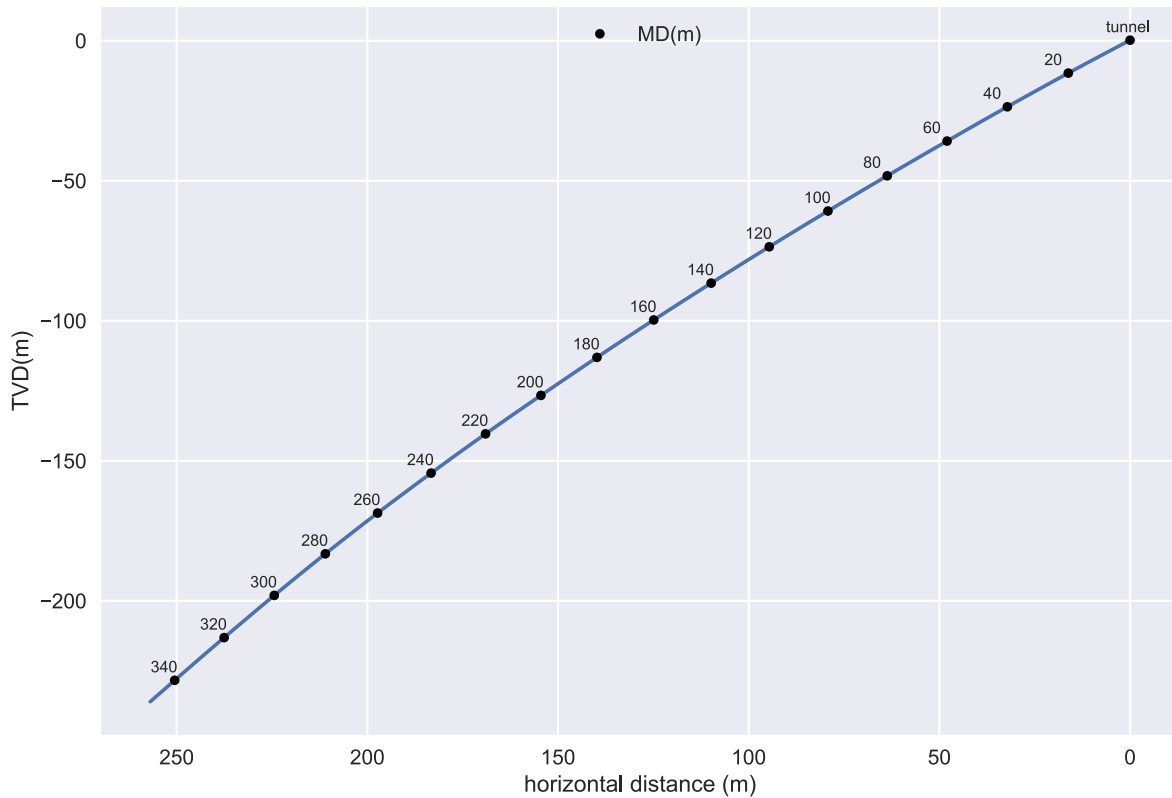
126

127

Figure 3. Diagram showing the disposition of well heads in the Bedretto Lab by March 2020. Taken from document from Zublin.

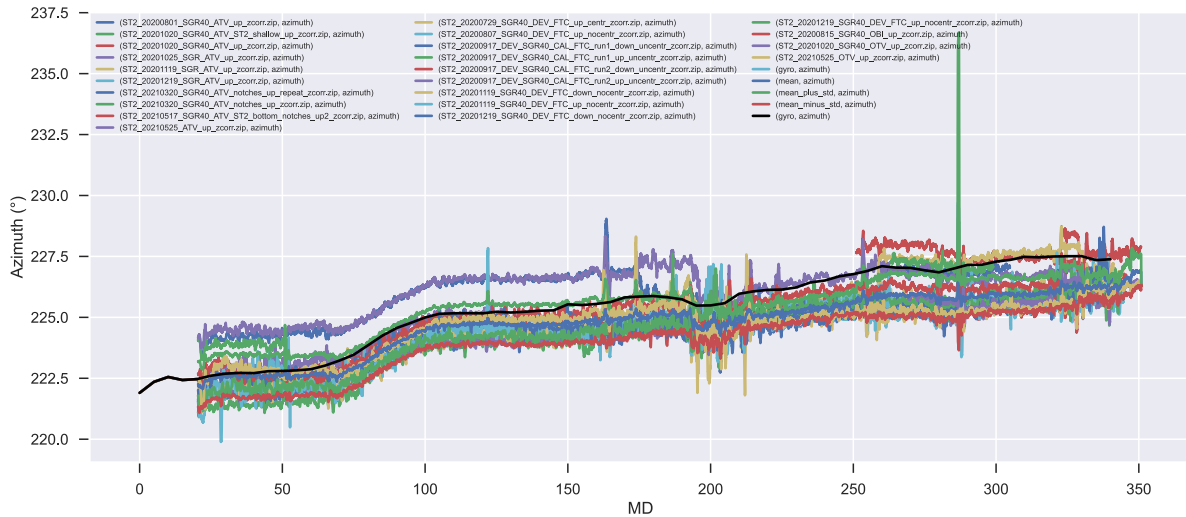
128

129 The inclination of the borehole diminishes from about 54° at the wellhead to approx. 40° at TD,
 130 meaning that the borehole gets steeper with depth. The azimuth is 222° at the wellhead and 227.5°
 131 at TD (Figure 4, Figure 5 and Figure 6).



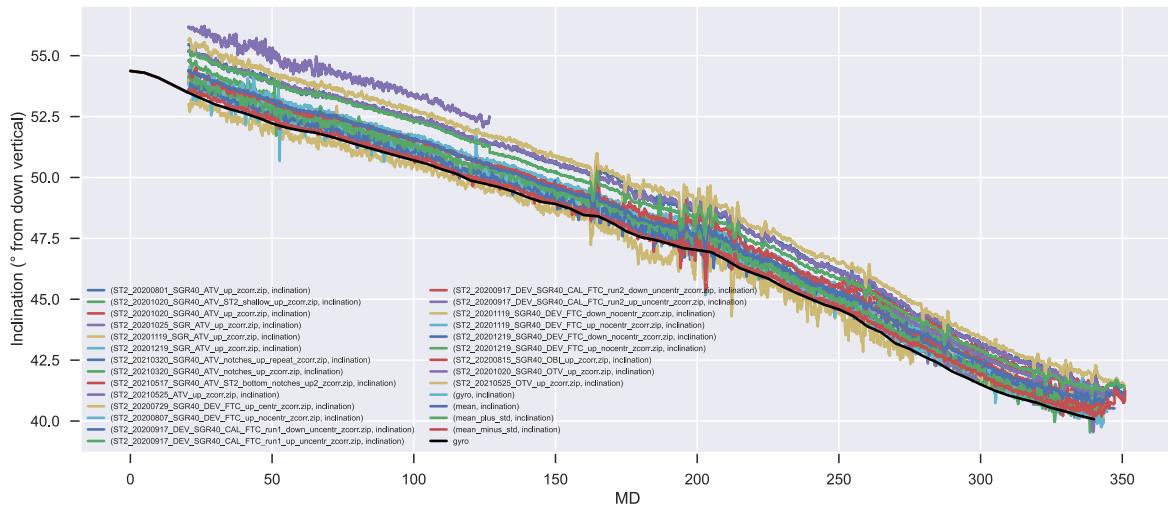
132
133

Figure 4. ST2 borehole path.



134
135
136
137

Figure 5. Azimuth (clockwise degrees from North) of ST2's path. Curves in color correspond to values from logging tools (ATV, OTV and DEV) with 2.21° added to correct for magnetic declination. The black curve is the gyro acquisition.



138

139 *Figure 6. Inclination (degrees from a vertical pointing down) of ST2's path. Curves in color correspond*
 140 *to values from logging tools (ATV, OTV and DEV) while the black curve is the gyro acquisition.*

141 The nominal diameter of the borehole is 8½ inches (below the conductor pipe). A non-calibrated
 142 caliper derived from the acoustic televiewer shows that the diameter is slightly wider at the top of
 143 the borehole (22.5cm instead of 21.6cm), and it diminishes with depth until it reaches the nominal
 144 value near TD (Figure 7). A regular borehole cross section can be observed between 50-160 m.
 145 Below 160m, regular cave-ins, breakouts and possible keyseats can be observed. Below 260m the
 146 cross section becomes relatively more regular although important irregularities in the borehole wall
 147 persist down to the TD.

148 Borehole breakouts are concentrated between 160-260m and 315-330m (Figure 7, Figure 8 and
 149 Figure 9). Figure 8 shows a rotation in the breakout's azimuth along the borehole depth. Zhang et al.
 150 (in press) describes in detail this rotation observed in ST2 as well as other boreholes in the BULGG.

151

152

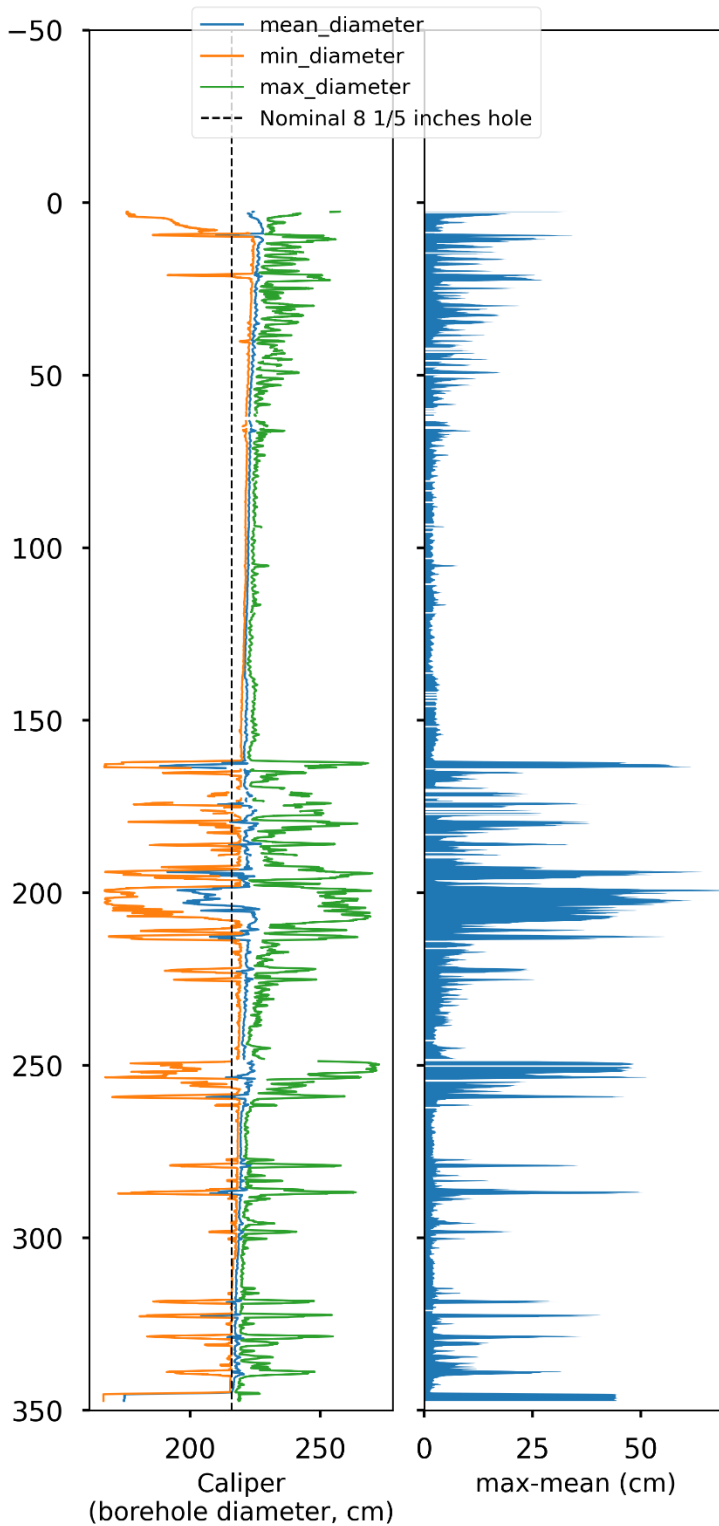


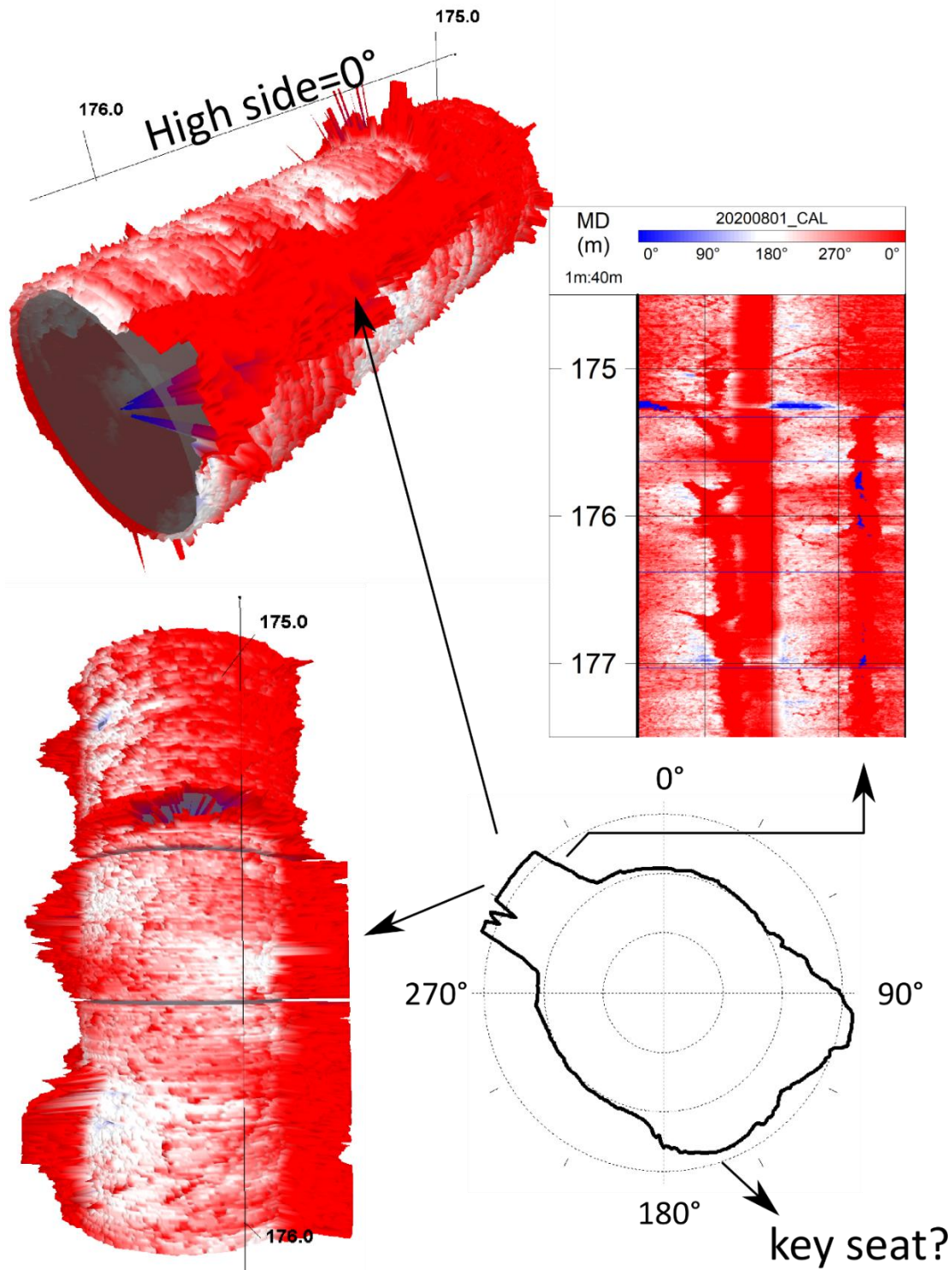
Figure 7. Caliper calculated from ATV log vs. Nominal diameter. The borehole gets narrower with depth. The section between 160 and 215m shows several cave ins. Sections with very low caliper values are certainly artifacts from the conversion of the acoustic signal.



154

155

Figure 8. Borehole breakouts in ST2



156

157 *Figure 9. Calculated caliper, 3D reconstruction and cross section view of breakouts between 175 and*
 158 *176 m MD. Breakouts are not exactly at 180° of each other. The breakout at around 100° rotates*
 159 *with depth until it reaches approx. 130°. The breakout at 310° stays fixed.*

160

161 3.2 Lithology

162 ST2, like all other boreholes in the Bedretto lab, was drilled through the Rotondo granite. The
163 Rotondo granite is composed of 64.9% of feldspars, 29.9% quartz and 5.2% of mafic minerals (Debon
164 & Lemmet, 1999). It presents a generally massive aspect with randomly distributed, large and easily
165 visible crystals that, in general, lack any consistent direction. Foliated zones are present but are
166 usually concentrated around individual shear (fault) zones.

167 Characterisation of the rock volume was carried out via core descriptions and an extensive campaign
168 of wireline logging. Figure 10 shows the major sections identified through the logging data:

- 169 ● Section A (0-155m): first section near the tunnel where fractures were identified in the
170 Optical televiewer (OTV) but that for the most part lack an acoustic response in the Acoustic
171 televiewer log (ATV). Spectral gamma ray (SGR) signal shows numerous peaks probably
172 indicating lithological heterogeneities in this section. Vp and Vs on the contrary are relatively
173 constant.
- 174 ● Section B (155-230m): A high deformation section about 80m thick where multiple fault core
175 zones are present and where the background fracture count increases considerably with
176 respect to the rest of the borehole. Borehole breakouts form almost exclusively in this
177 section. The SGR signal is more heterogenous and varies with higher frequency. Vp and Vs
178 show also larger amplitude variations.
- 179 ● Section C (230-300m): shows individual and “isolated” fault core zones with strong acoustic
180 response intercalated with sections of low fracture count. Spectral gamma is more regular
181 than in section B.
- 182 ● Section D (300-350m): Towards the bottom of the borehole, the granite looks clearer in the
183 OTV in comparison to the rest of the borehole. The total gamma ray shows a base level that
184 is consistently higher than the sections above. These observations point to a section of the
185 granite that is most probably richer in Feldspars. Structures in the shallowest 20m of this
186 section have a smaller amplitude response than those towards the deepest 30m.

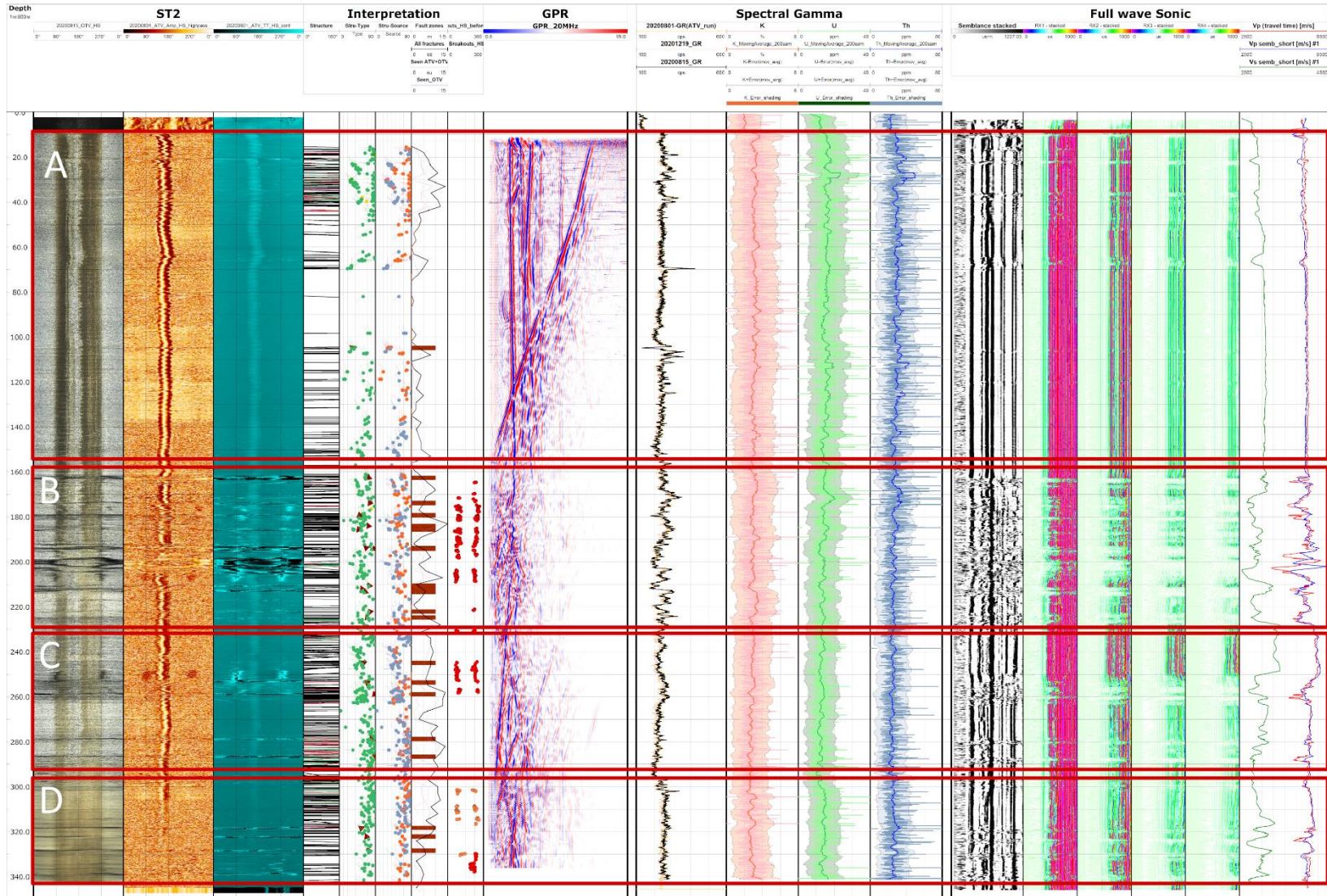
187 Except for some shallow hydrotests and notching between 150m and 300m, all other activities
188 presented in this report were carried out in the deepest part of section C (275m-300m) or entirely in
189 section D (300m-350m).

190

191

192

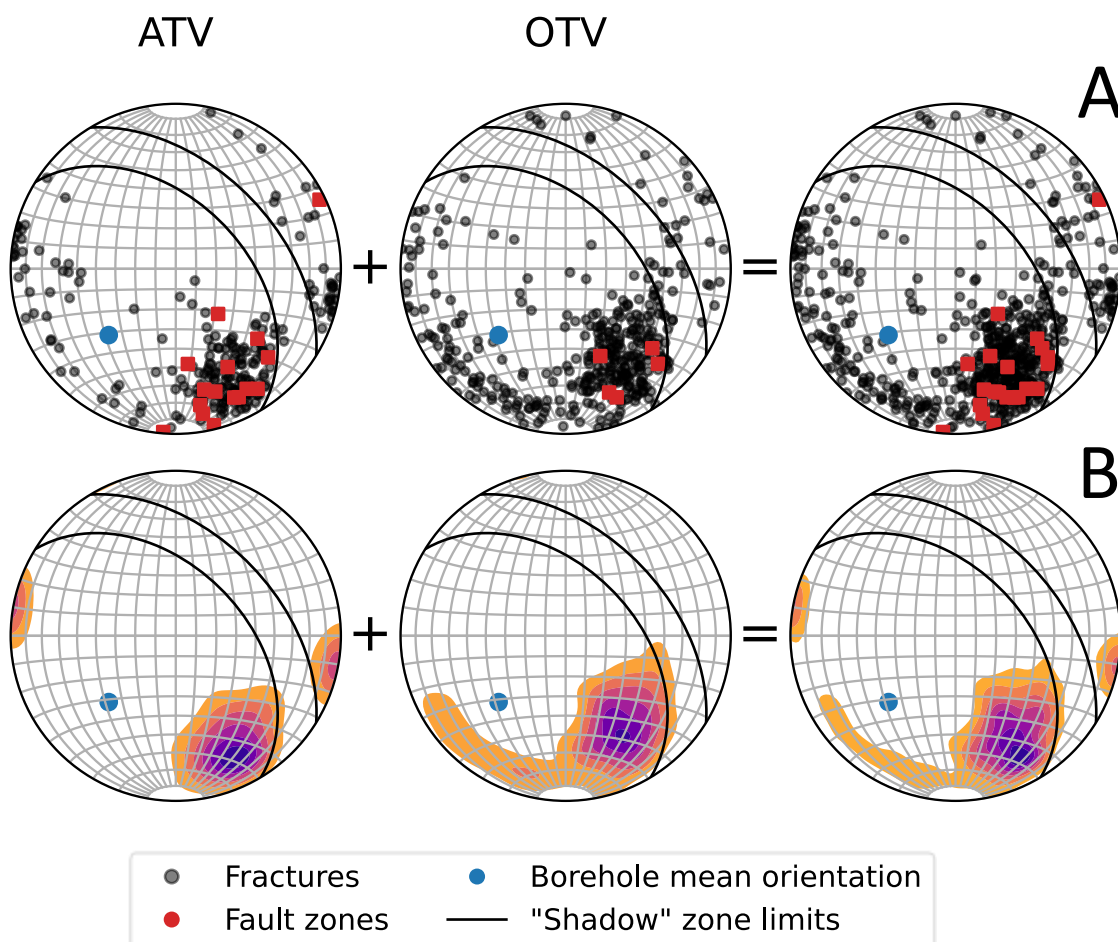
193 *Figure 10 Next Page. Composite data log of ST2 with Optical televiewer (OTV), Acoustic televiewer*
194 *(ATV), structural interpretation, borehole GPR, spectral gamma and full-wave sonic.*



196 3.3 Structure

197 Structures were interpreted in the acoustic and optical televiwers (ATV and OTV) and were
 198 classified as either "generic fractures" or "fault zones". Other structure types were identified but can
 199 be considered here as negligible because of their scarcity in the logs (e.g. quartz veins). A detailed
 200 analysis of the structure for the whole BULGG can be found in the report "Structural characterization
 201 of the Bedretto Underground Laboratory for Geoenergies (BULGG)" by R. Castilla.

202 Measured orientations concentrate mainly around strikes= $N140^{\circ}$ - 150° and dips= 40° - 60° . Secondary
 203 directions include one concentrated around strike= $N10^{\circ}\pm 5^{\circ}$, dip= $90^{\circ}\pm 5^{\circ}$ and a disperse one of SE-
 204 NW striking structures identified mainly in the OTV. Generic fractures can be found in all these 3
 205 groups while most fault zone cores are only found in the NE-SW group dipping NW.



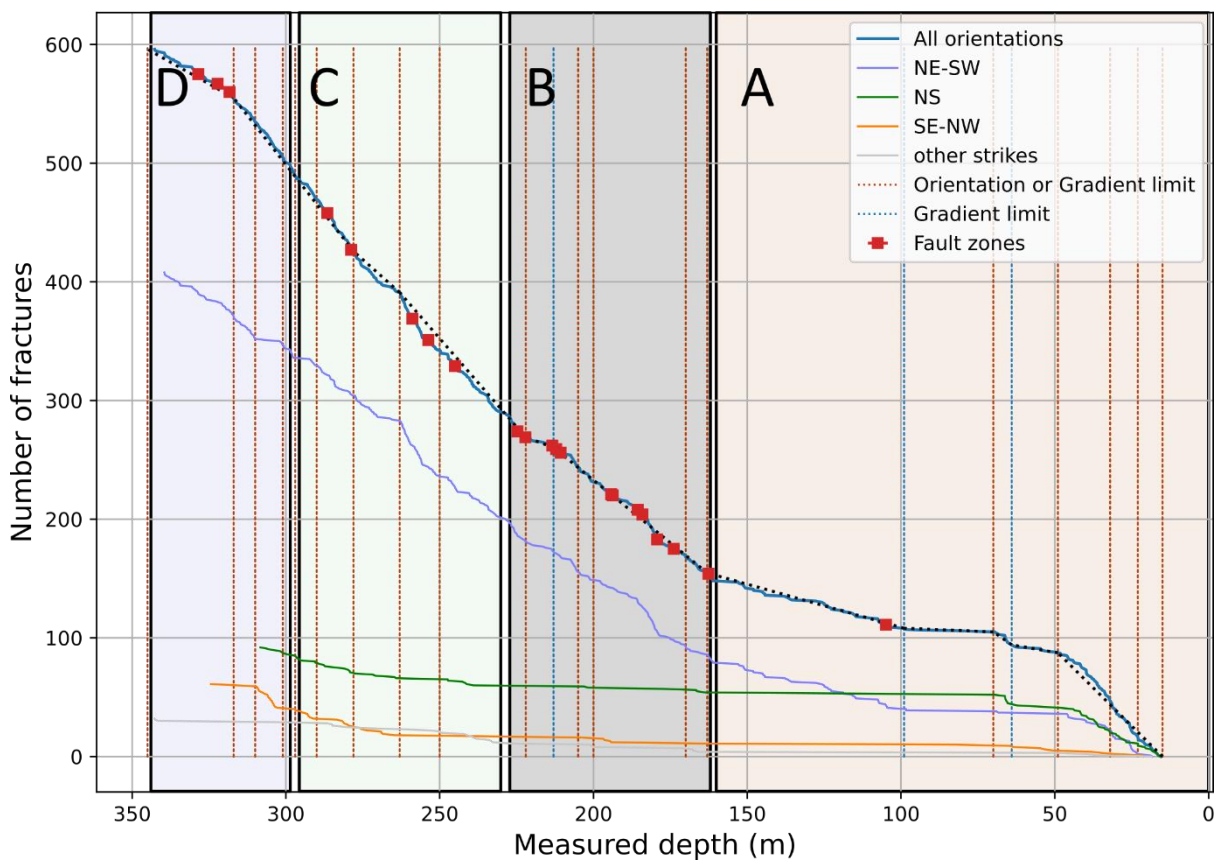
206

207 *Figure 11. Structures interpreted in the televiwer logs. A) Poles to structure planes, B) Contours of*
 208 *pole density.*

209 The region where under sampling of structures is expected to occur (aka "shadow zone") is indicated
 210 in Figure 11 by the area between two black polylines. This data gathering pitfall is common to all
 211 structural work and is formally known as the orientation bias. A correction, only relevant for
 212 quantitative workflows (e.g. construction of a DFN model) can be applied to correct the
 213 frequency/spacing of measured data. This correction is not useful for descriptive reports like the

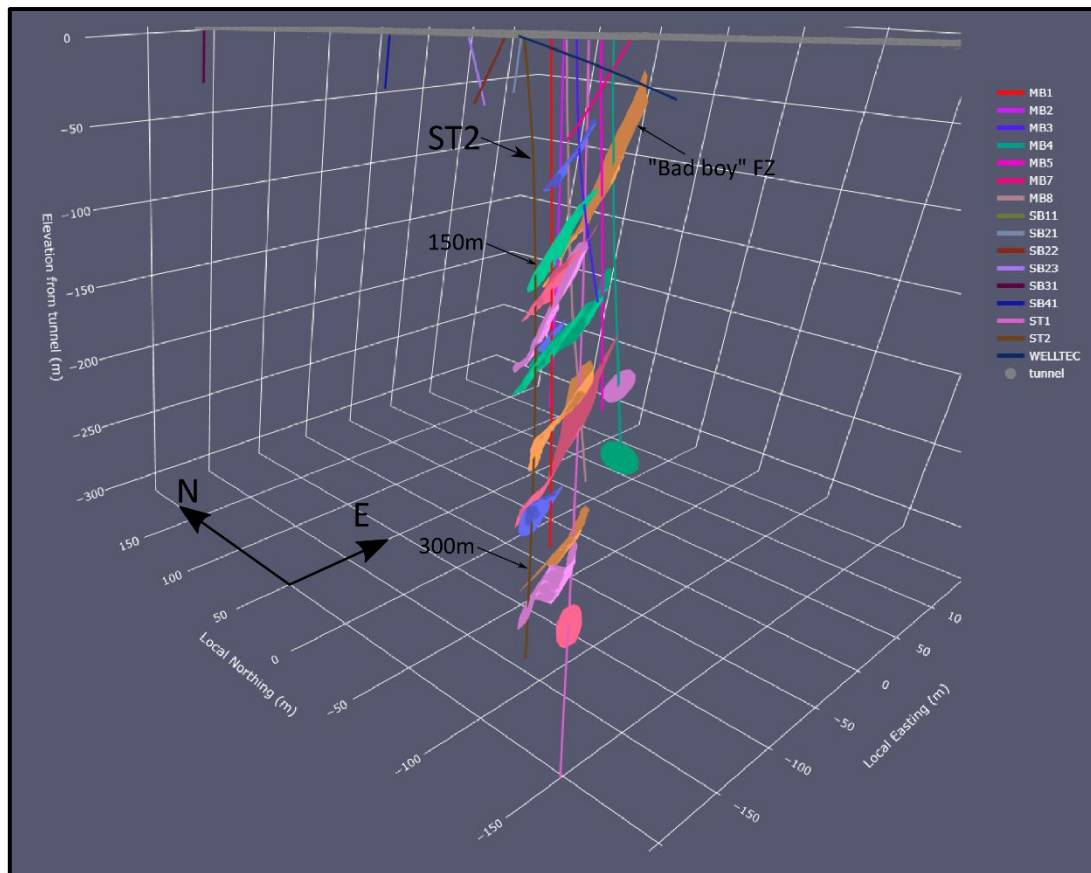
214 present one. No reliable processing method exists to "populate" the shadow zone. The two polygons
 215 in Figure 11 mark the zone where planes forming less than 20° with the borehole axis would plot.
 216 This theoretical shadow zone fits well with the lack of data points in that area of the stereonets. For
 217 the qualitative and descriptive purpose of this report no correction of the orientation bias was
 218 deemed necessary.

219 The frequency of structures occurrence along the borehole is shown in Figure 12. Fault core zones
 220 are marked with a red square. The lithological subunits identified through the log integration (Figure
 221 10) is shown as lightly colored rectangles. The total structure count curve ("All orientations" in Figure
 222 12) mimics the count of structures in the NE-SW set (light blue curve). The NS set is only present at
 223 the shallow and deep ends of the borehole while SE-NW set is only present in the deepest 90m.



224
 225 *Figure 12. Structure frequency for the total population and detailed for each individual orientation*
 226 *set.*

227 Fault zones identified in ST2 were correlated with those interpreted in other boreholes in the
 228 BULGG. A 3D view with the resulting fault surfaces is shown in Figure 13. All faults in ST2 connect up
 229 dip with other boreholes.



230

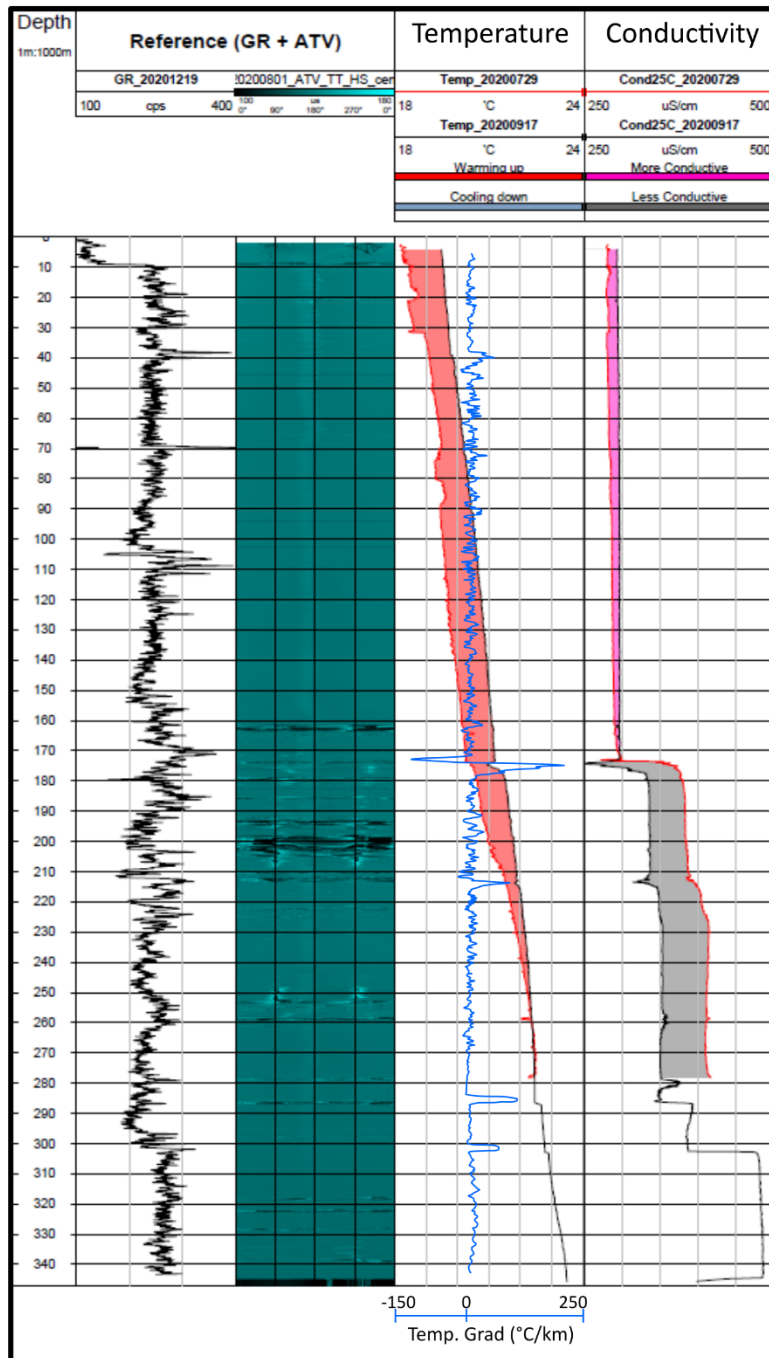
231

Figure 13.

232 3.4 Fluids

233 Fluid and conductivity of the fluid in the borehole were extensively monitored through logging
 234 (Table 1 and Figure 15). Comparison of a log acquired just before the final stage of drilling
 235 (29/07/2020) and another one run 1½ months after (17/09/2020), shows how the fluid in the
 236 borehole gets warmer with time meaning that the in-situ fluid is warmer than the circulated fluid
 237 during drilling. Conductivity shows changes in time as well, but they differ depending on the position
 238 in the borehole. Above 175m the fluid got slightly more conductive (i.e., salinity increased) with time
 239 while below the conductivity decreased significantly.

240 A temperature gradient was estimated using a rolling window of 2m on the September 17th log. An
 241 average gradient of about 11.5 °C/km was estimated with important anomalies around 175m, 215m
 242 and 285m (Figure 14). Smaller anomalies can also be seen at 40m and 305m. Simultaneous
 243 temperature and conductivity anomalies can be observed at 175m, 215m, 285m and 305m.



244

245 *Figure 14. Temperature and conductivity logs acquired in ST2 towards the end of drilling*
 246 *(29/07/2020) and about 1½ months afterward (17/09/2020).*

247 **4. Summary of activities in the framework of ZoDrEx**

248 Table 1 and Figure 15 show the history of activities carried out in ST2, from its drilling to the final
 249 stimulation in the framework of ZoDrEx. From spudding until the last stimulation, the works were
 250 conducted along 15 months. In this span of time, 14 intervals were the object of hydraulic tests, 20

251 minifrac tests were conducted and 18 intervals were stimulated by hydraulic injection. In addition, 4
252 notching campaigns were carried out on both, open hole and cased & cemented configurations. 25
253 televiwer logs were acquired (19 ATV and 6 OTV) in addition to 15 temperature and conductivity
254 logs. The rock volume below 300m was the most repeatedly tested and stimulated

255

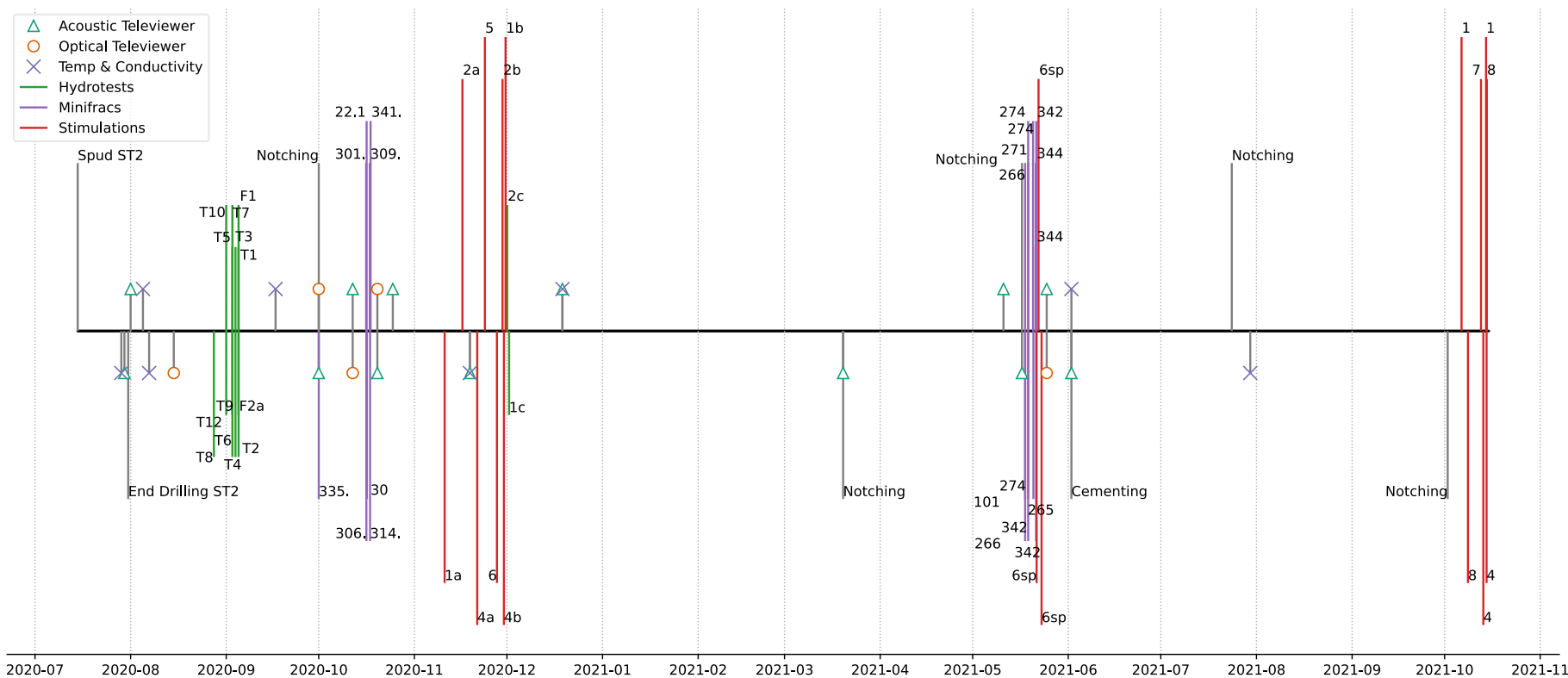
256 Table 1 Summary of operations carried out in ST2 257

Date	Borehole	Action
14/07/2020	ST2	Spud
29/07/2020	ST2	FTC
29/07/2020	ST2	FTC
30/07/2020	ST2	ATV
31/07/2020	ST2	End Drilling
01/08/2020	ST2	ATV
01/08/2020	ST2	ATV
05/08/2020	ST2	FTC
07/08/2020	ST2	FTC
15/08/2020	ST2	OTV
28/08/2020	ST2	Start Hydrotesting campaign
07/09/2020	ST2	End Hydrotesting campaign
14/09/2020	ST2	Start FO-DTS campaign
17/09/2020	ST2	End FO-DTS campaign
17/09/2020	ST2	FTC
21/09/2020	ST2	Start Notching campaign
01/10/2020	ST2	End Notching campaign
01/10/2020	ST2	ATV
01/10/2020	ST2	OTV
12/10/2020	ST2	ATV
12/10/2020	ST2	OTV
16/10/2020	ST2	Start Mini-Frac campaign
17/10/2020	ST2	End Mini-Frac campaign
20/10/2020	ST2	ATV
20/10/2020	ST2	ATV
20/10/2020	ST2	OTV
20/10/2020	ST2	OTV
25/10/2020	ST2	ATV
09/11/2020	ST2	Start Stimulation campaign
19/11/2020	ST2	ATV
19/11/2020	ST2	ATV
19/11/2020	ST2	FTC
19/11/2020	ST2	FTC
30/11/2020	ST2	End Stimulation campaign

258

Date	Borehole	Action
19/12/2020	ST2	ATV
19/12/2020	ST2	FTC
19/12/2020	ST2	FTC
10/03/2021	ST2	Start Notching campaign
18/03/2021	ST2	End Notching campaign
20/03/2021	ST2	ATV
20/03/2021	ST2	ATV
11/05/2021	ST2	Start Notching campaign
17/05/2021	ST2	End Notching campaign
17/05/2021	ST2	ATV
17/05/2021	ST2	ATV
18/05/2021	ST2	Start Mini-Frac campaign
21/05/2021	ST2	End Mini-Frac campaign
21/05/2021	ST2	Start Re-Stimulation campaign
23/05/2021	ST2	End Re-Stimulation campaign
25/05/2021	ST2	ATV
25/05/2021	ST2	OTV
25/05/2021	ST2	Start Casing installation - Cementation
02/06/2021	ST2	End Casing installation - Cementation
20/07/2021	ST2	Start Notching campaign 1
30/07/2021	ST2	End Notching campaign 1
30/07/2021	ST2	FTC
30/07/2021	ST2	FTC
30/07/2021	ST2	FTC
13/09/2021	ST2	Start Notching campaign 2
02/10/2021	ST2	End Notching campaign 2
04/10/2021	ST2	Start Stimulation campaign
15/10/2021	ST2	End Stimulation campaign
ATV = Acoustic Televiewer; OTV = Optical televiewer		
FTC = Fluid temperature & Conductivity		

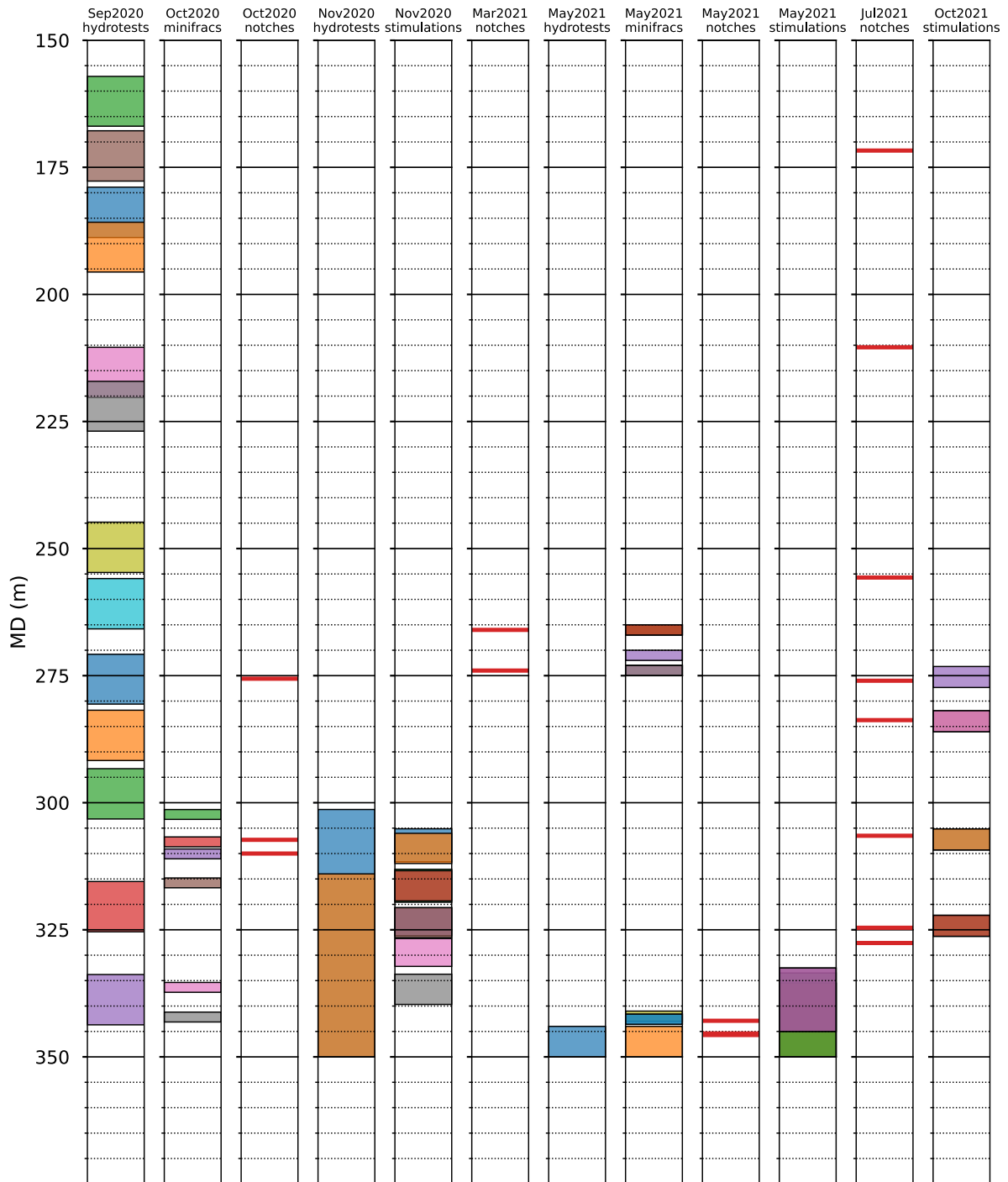
259



260

261

Figure 15. Timeline of operations on ST2



262

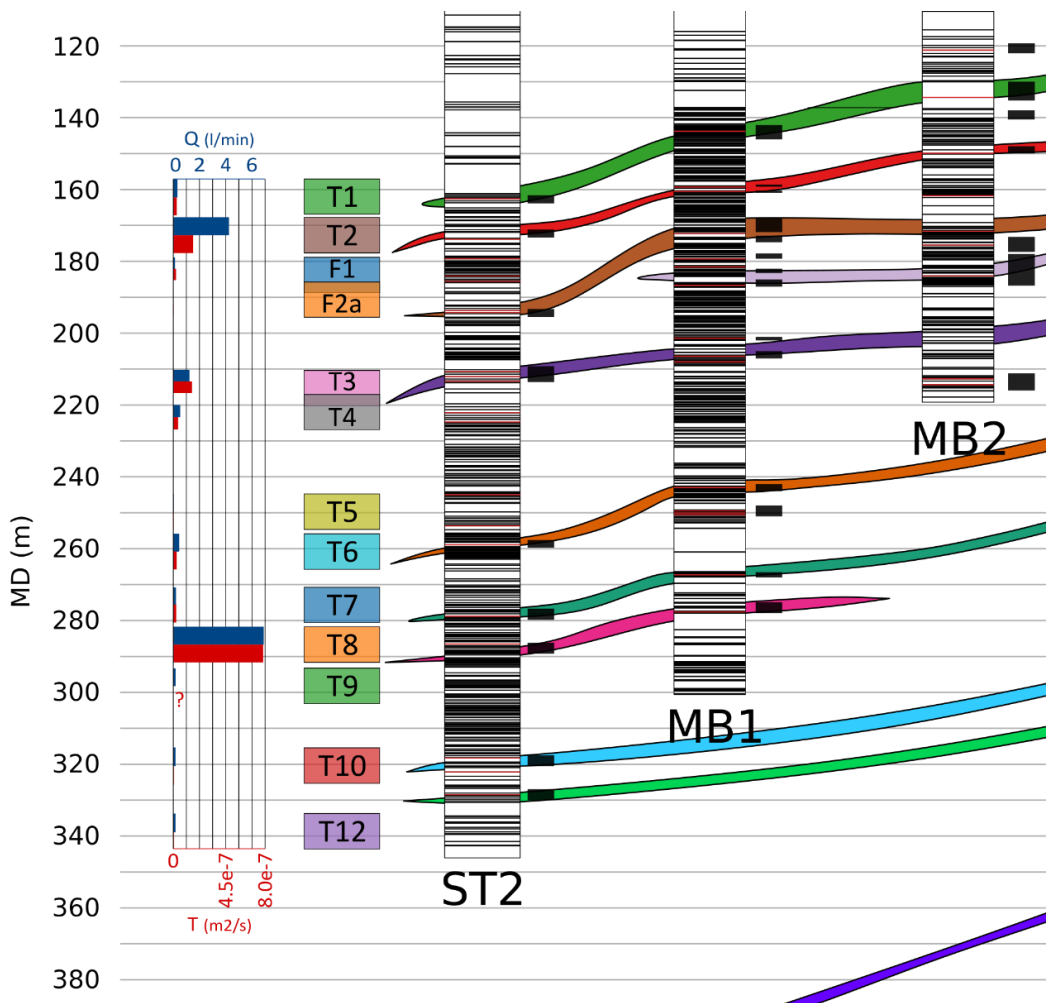
263 *Figure 16. Depth intervals where different hydraulic tests, minifrac, stimulations and notching were*
 264 *carried out. Colors are random and are only intended to improve the readability of the plot*
 265 *Hydraulic tests*

266 5. Hydrotests

267 Formation pressure and flow rates were extensively measured in ST2 below 160m. A first campaign
 268 of measurements was carried out between August and September 2020, testing a total of 13
 269 intervals (Figure 17 and Figure 16). A second set of measurements was carried out in December 2020
 270 with a single packer setting to isolate the bottom section of the borehole (Figure 16). Detailed
 271 analysis of these tests is available in the ZoDrEx report "Evaluation of hydraulic tests in borehole
 272 ST2" by Meier et al.

273 Figure 17 shows the results of these hydraulic tests alongside the structural log and fault zone
 274 correlation with nearby wells. Three intervals stand out with important flow rates and estimated
 275 transmissibility:

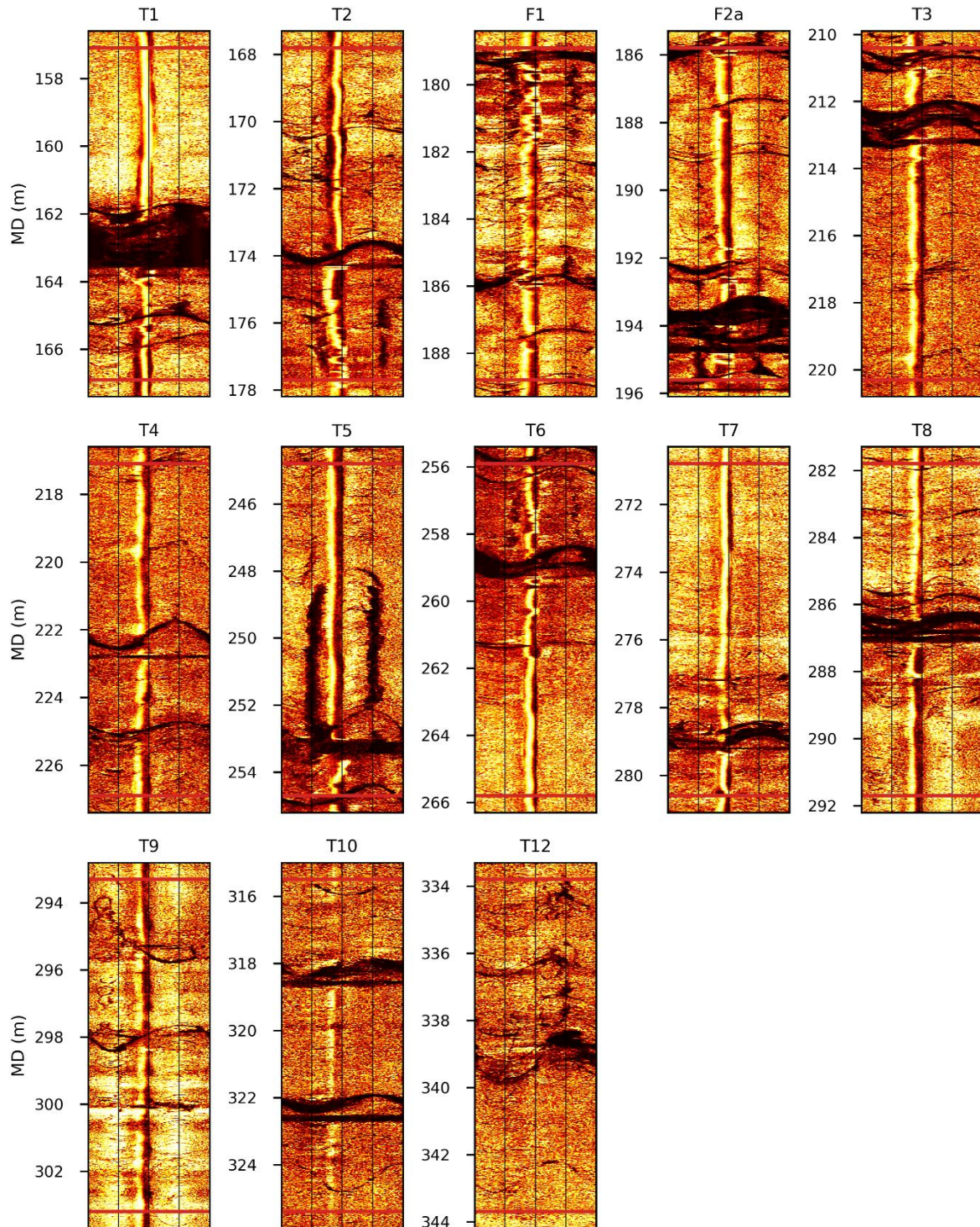
- 276 1. T8: Flow=6.90 l/min; Transmissibility=7.7e-7 m2/s
- 277 2. T2: Flow=4.25 l/min; Transmissibility =1.7e-7 m2/s
- 278 3. T3: Flow =1.24 l/min; Transmissibility =1.6e-7 m2/s



279

280 *Figure 17. Hydraulic tests results and structural correlation between boreholes in the BULGG.*

281 Important structures can be identified in each tested interval (Figure 18). There doesn't seem to be
 282 significant differences that could explain the variability in hydraulic properties in terms of thickness,
 283 orientation, or total number of structures. It is likely that the observed variability in hydraulic
 284 properties is linked to the way the structural network is connected beyond the borehole wall.



285

286

Figure 18. ATV log for each hydrotest interval.

287 **6. Notching**

288 Notches are micro-drills performed at the borehole wall. They show up as circular or elliptical
 289 shaped features in borehole images. In terms of acoustic signal, notches show a response similar to
 290 any other irregularity in the borehole wall (i.e. fractures, breakouts), that is longer travel times and
 291 lower amplitudes.

292 Notching of the borehole wall has several positive effects:

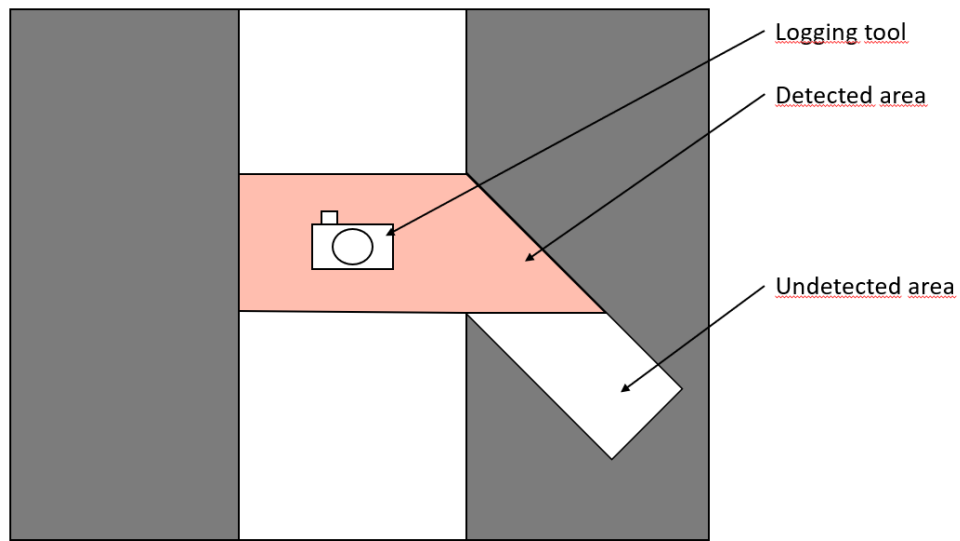
- 293 • It may help promoting transverse fractures during hydrofrac operations.
- 294 • Decrease near-wellbore tortuosity.
- 295 • Might help mitigate seismic risks by reducing the pressure required for breakdown

296 In the context of ZoDrEx, 4 notching campaigns were carried out with a total of 16 depths perforated
 297 (Table 2). Since the micro-drills are inclined at 60° with respect to the borehole axis, the imaging of
 298 notches by televiewer logs is limited to the first millimeters of the perforations (Figure 19). A 3D
 299 reconstruction (Figure 20) helps understand this factor that limits the capacity to evaluate the final
 300 geometry of each notch.

301 *Table 2. Summary of notching operations.*

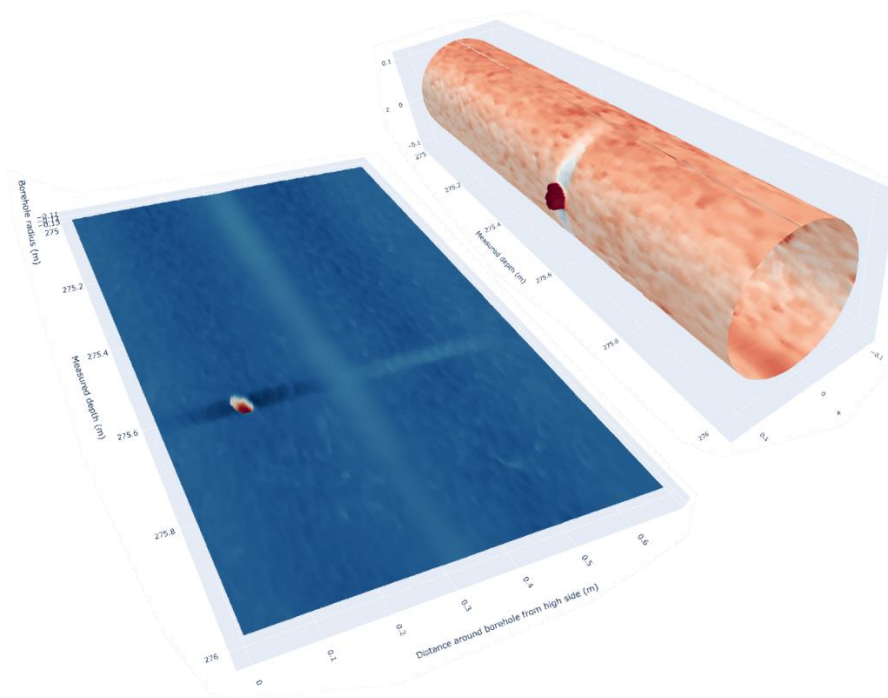
Notching		
Date	MD (meters)	Location (Degrees from the borehole high side)
01.10.2020	275.6	75°
	307.3	7°
	310.0	300°
20.03.2021	266.0	50°-70°-123°-170°257°
	274.0	132°-194°-238°260°320°
17.05.2021	342.9	33°-80°-340°
	345.4	115°-165°-205°-295°
	345.7	285°-340°
20.07.2021-02.10.2021	171.7	180°-270°
	210.4	270°-235°
	255.7	270°
	276	290°-270°
	283.75	305°
	306.5	250°
	324.6	272°
	327.6	unsuccessful

302



303
304
305

Figure 19. Imaging of notches at oblique angle with borehole are incomplete. Image courtesy of Niklas Geissler.



306
307
308

Figure 20. 3D reconstruction of ST2 around 275m MD showing, partially, the notch at 275.6m. The total length and complete geometry of the notch is obscured by the inclination of the perforation.

309 **6.1 October 2020**

310 Three perforations were carried out at different depths in the borehole between 275m-310m. The 3
311 notches sit close to isolated natural fractures with limited acoustic response.

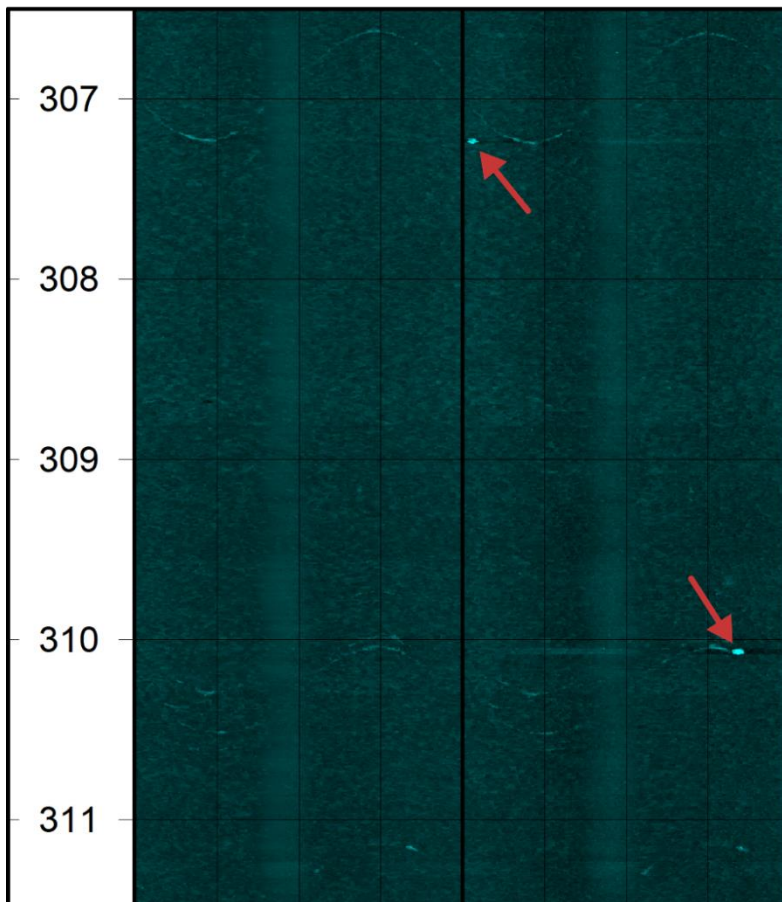
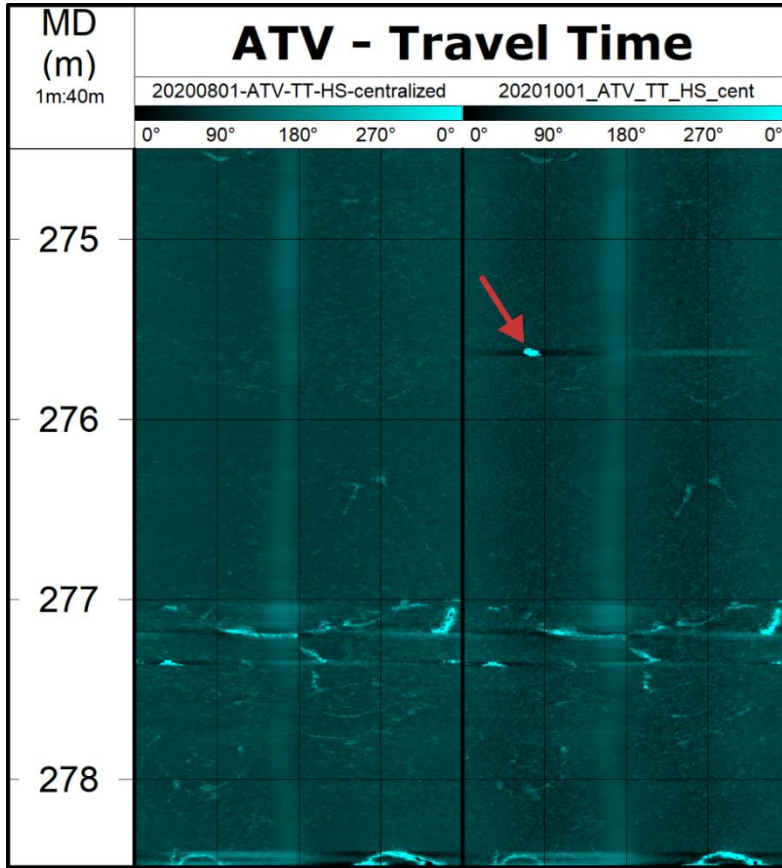
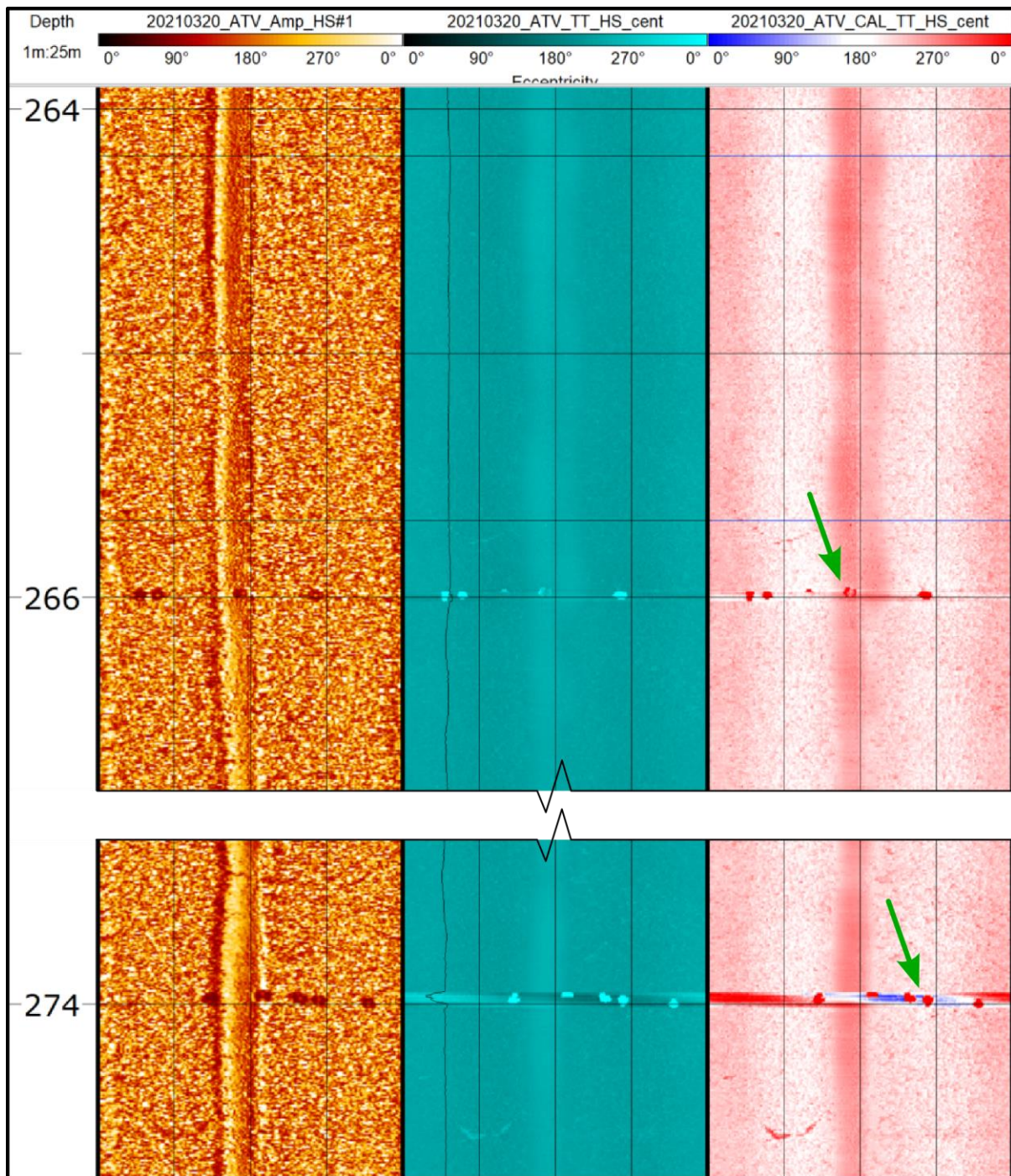


Figure 21. Examples of notching from October 2020 observed on ATV log (travel time).

312 6.2 March 2021

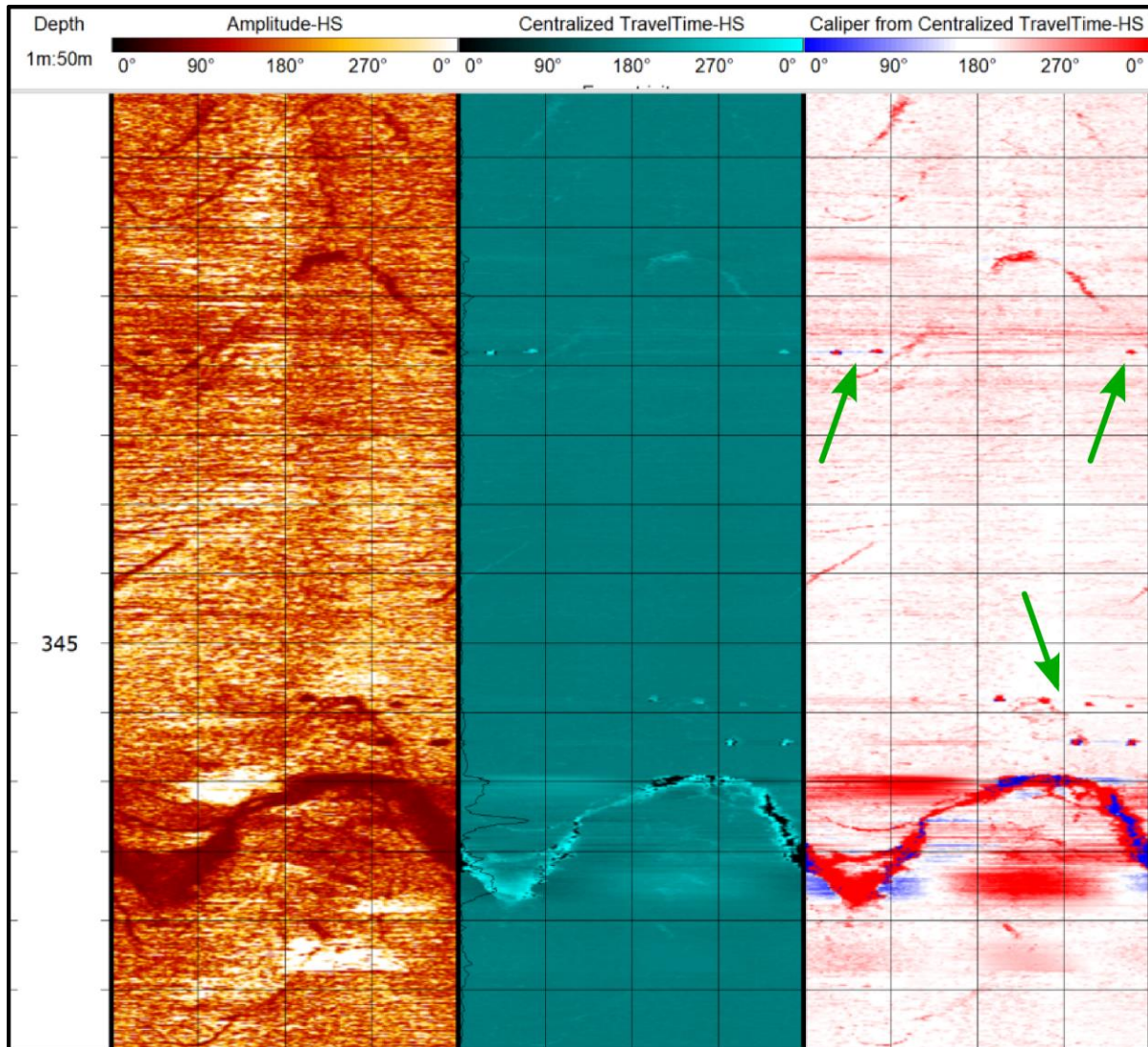


313

314

Figure 22. Result from notching operations carried out in March 2021.

315 6.3 May 2021



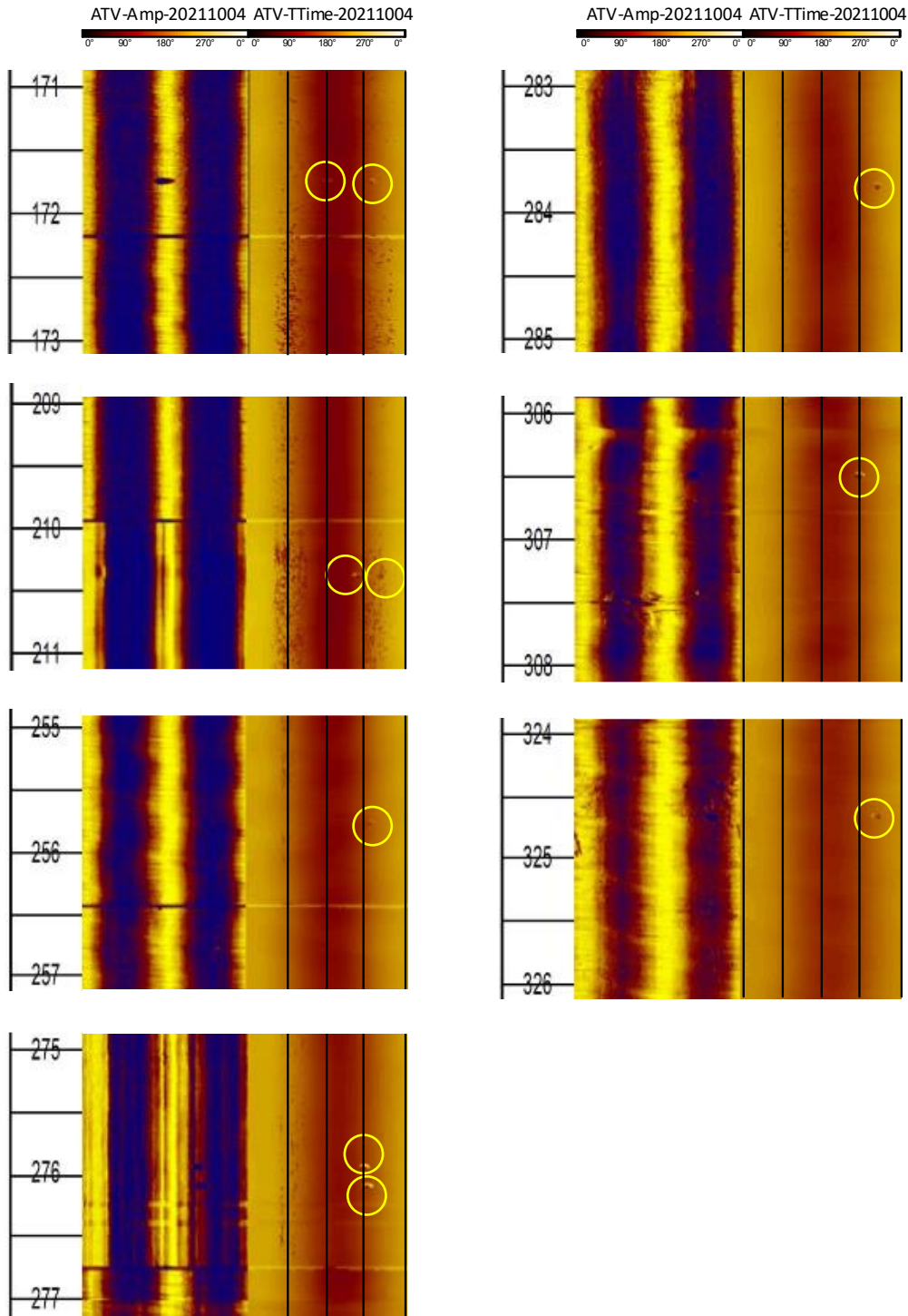
316

317

Figure 23. Result from notching treatment in May 2021

318 6.4 July-October 2021

319 A notching campaign through the cased and cemented borehole wall was carried out between July
 320 and October 2021. Seven depths were successfully perforated between 171-276m. All perforations
 321 are in the southern side of borehole between angles 180-305° from the high side (Figure 24).



322

323

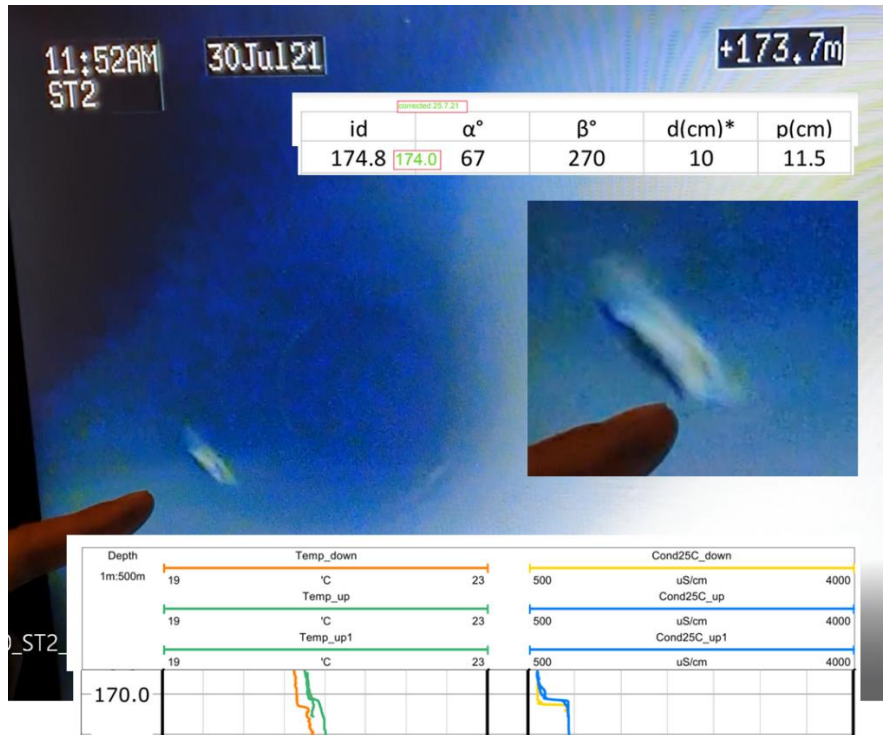
Figure 24. Notches through the casing drilled between July and October 2021.

324

A camera run allowed to check the depth of these notches and a match with fluid temperature and conductivity responses associated to the notching (). A certain mismatch exists between the depths shown in the camera runs, the ATV and the FTC logs. This mismatch is inherent to the logging process due to the different characteristics of the logging tools and the cables attached to them. In open hole conditions this mismatch is easily corrected, and all logs are corrected to match a unique

328

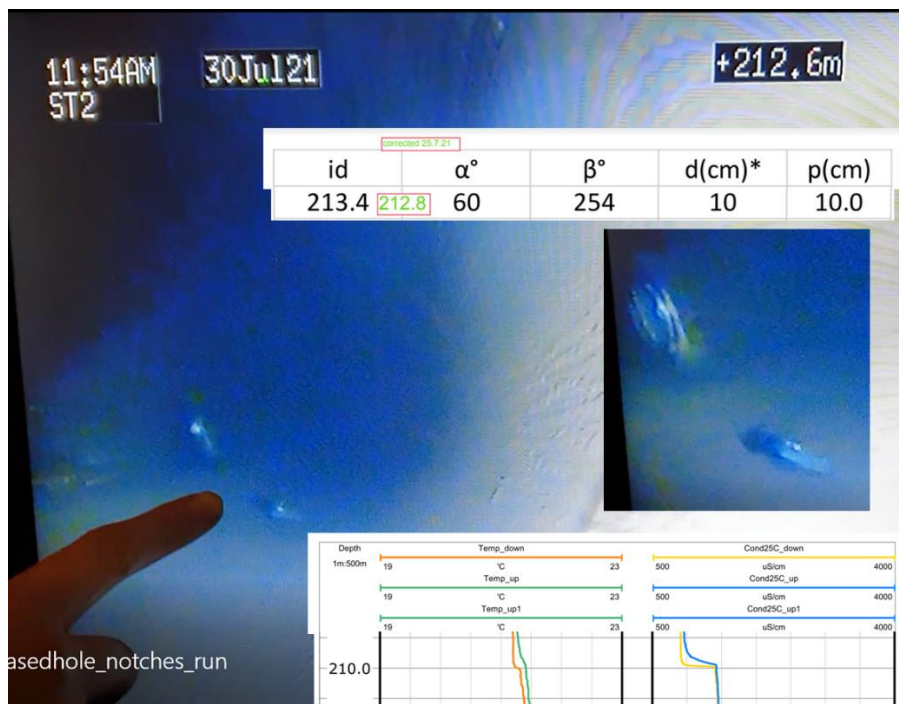
329 reference log. The lack of visible features in the cemented borehole wall makes this correction
 330 impossible so the depths mismatches persist.



331

332

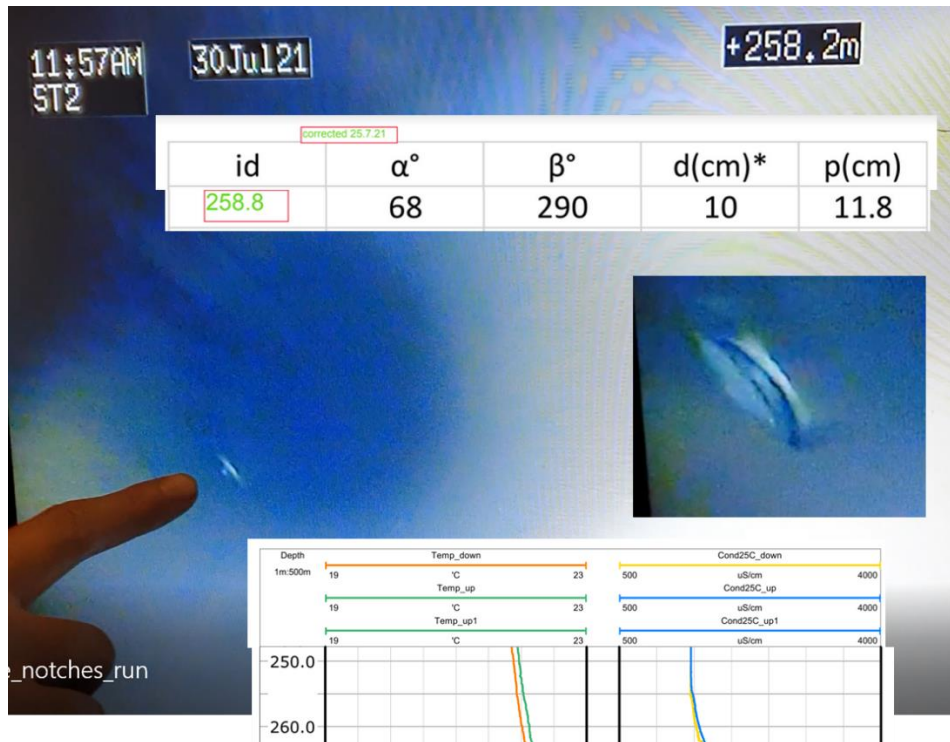
Figure 25. Notches listed in Table 2 at 171.7m.



333

334

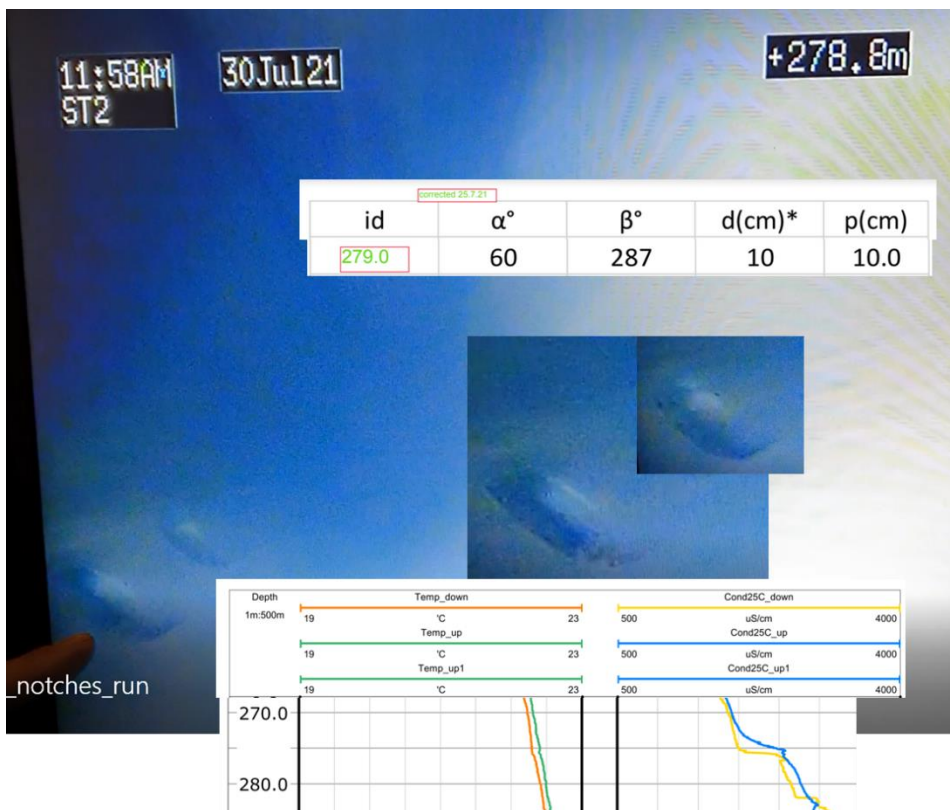
Figure 26. Notches listed in Table 2 at 210.4m.



335

336

Figure 27. Notches listed in Table 2 at 255.7m.



337

338

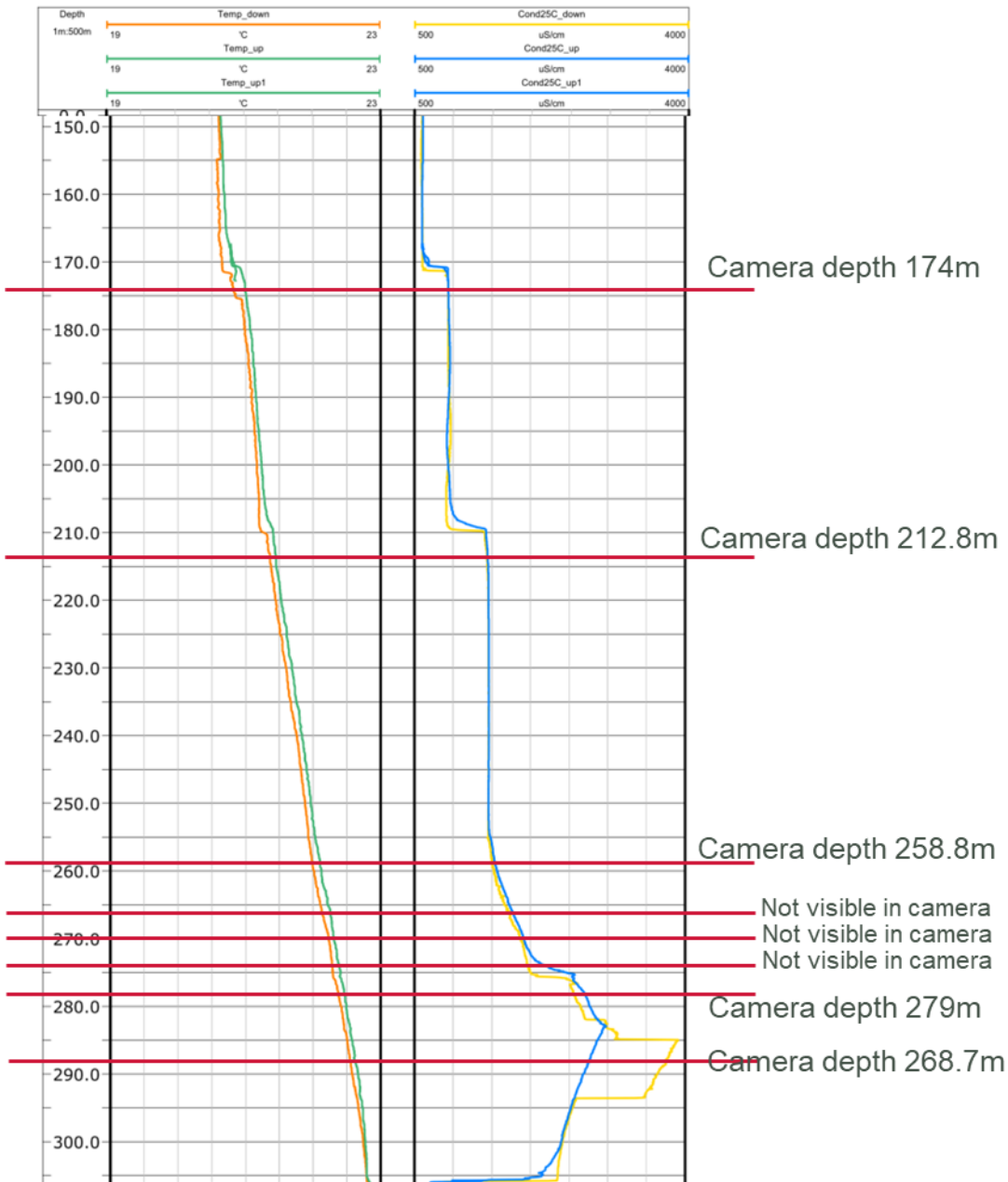
Figure 28. Notches listed in Table 2 at 276m.



339

340

Figure 29. Notches listed in Table 2 at 283.75m.

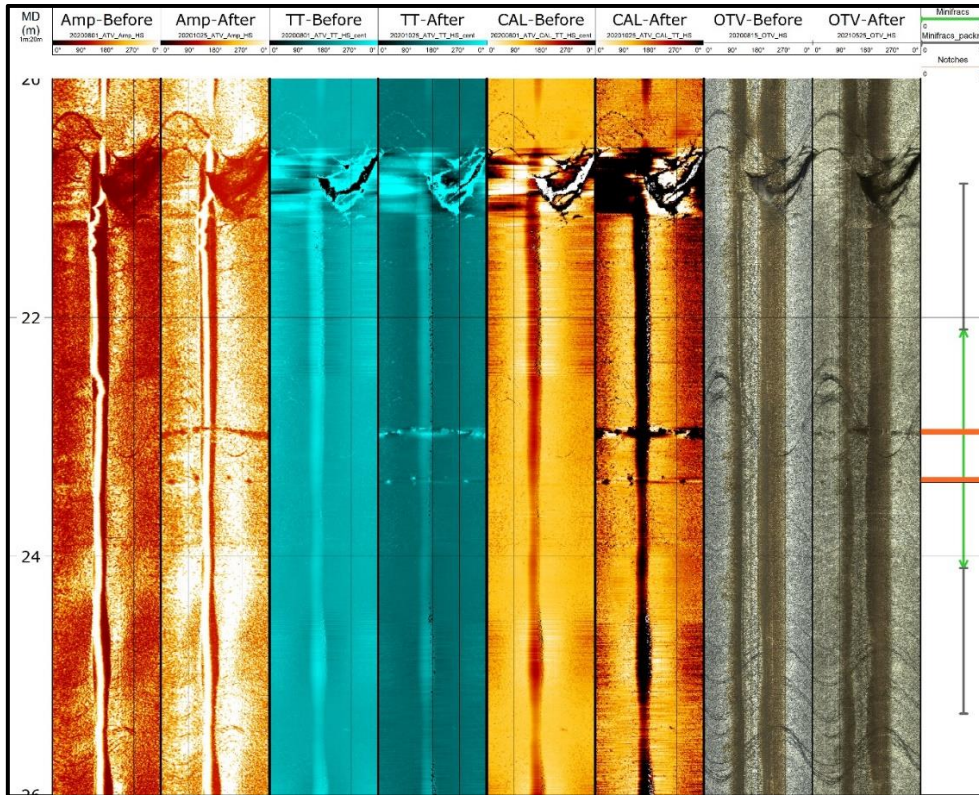


341

342 *Figure 30. Summary of notches identified in the camera run and the associated fluid temperature and*
 343 *conductivity response.*

344 7. Minifrac – October 2020

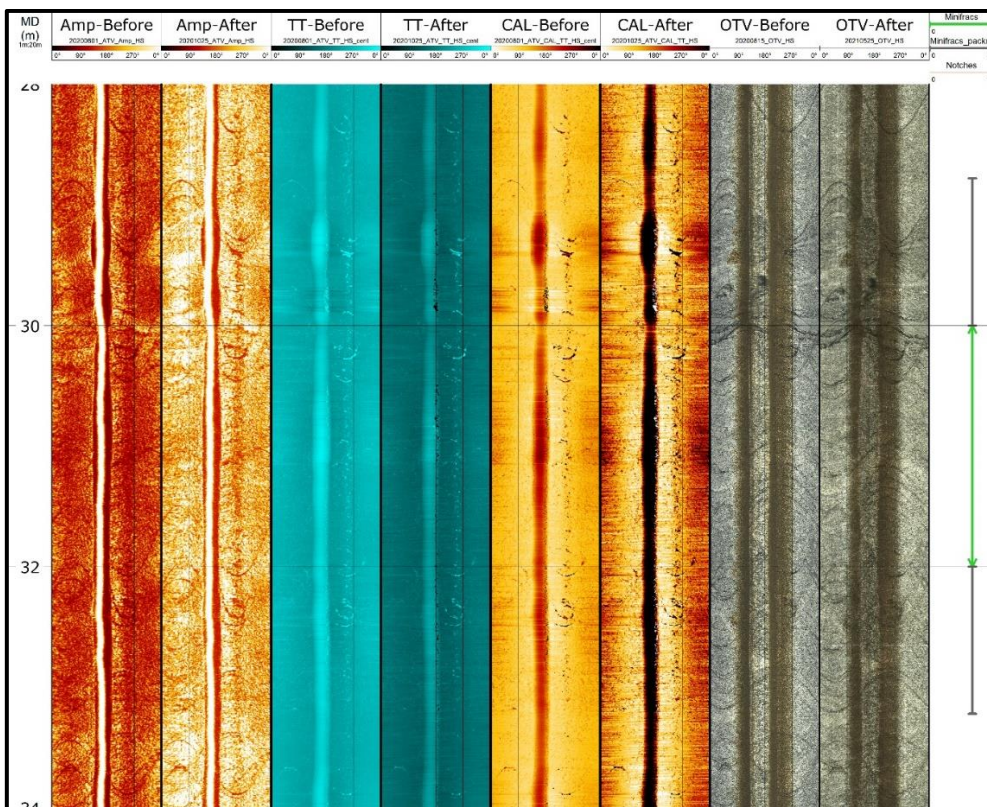
345 Minifrac tests were carried out in 8 intervals along ST2. No tensile fractures were identified on image
 346 logs acquired after the tests. OTV logs show that all minifrac were done in intervals with pre-
 347 existing natural fractures that, for most of them, lack of any clear amplitude signal (i.e. they don't
 348 show up in ATV logs). So, despite their original "tight" state, the minifrac tests most probably
 349 managed to jack these structures instead of creating new tensile fractures (Figure 31 to Figure 37).



350

351

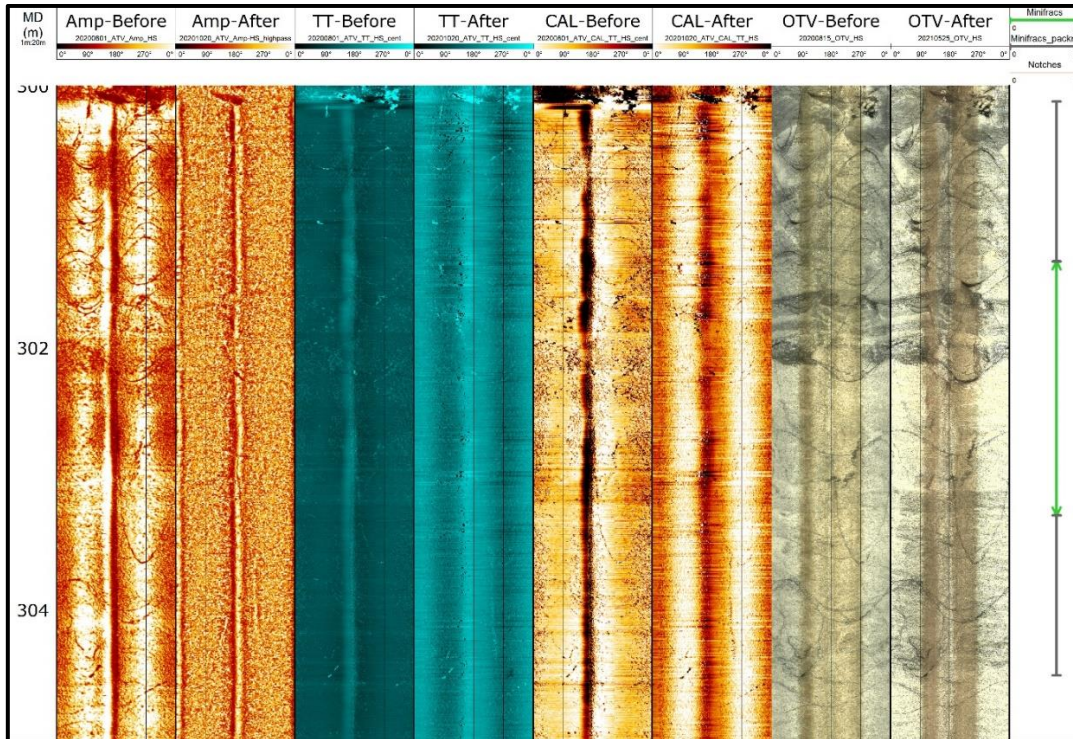
Figure 31. Interval 22.1-24.1m.



352

353

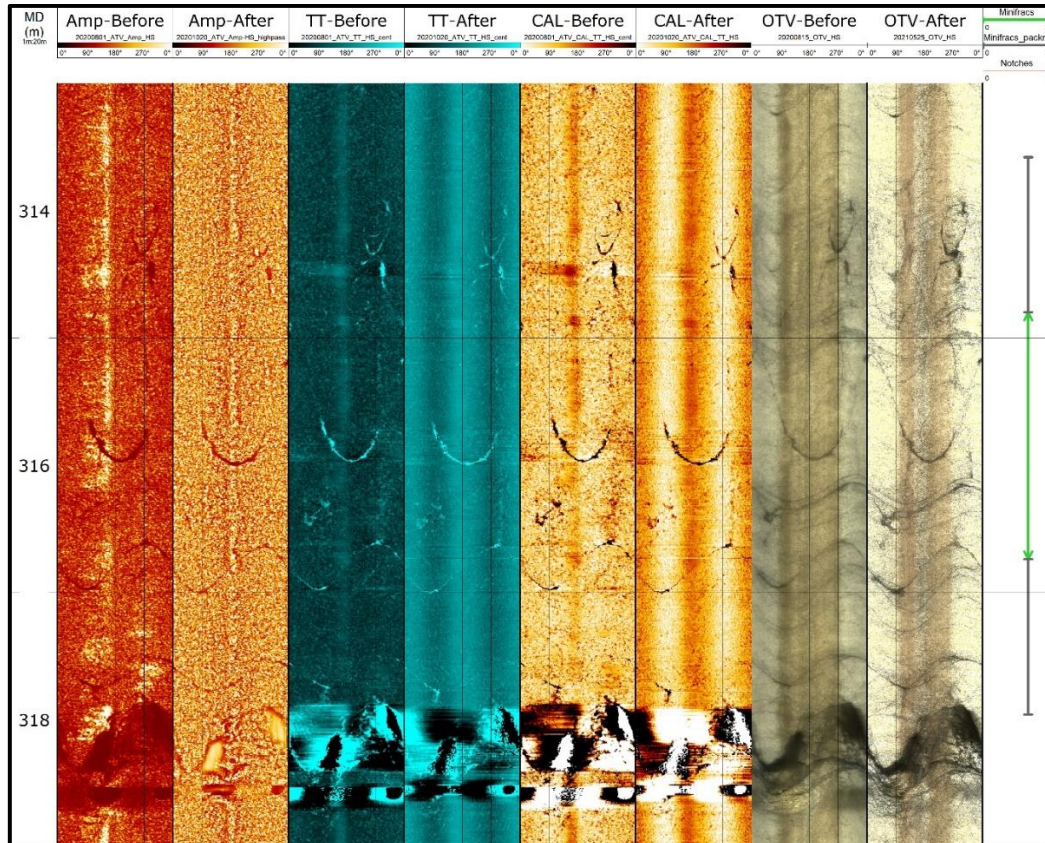
Figure 32 Interval 30-32m



354

355

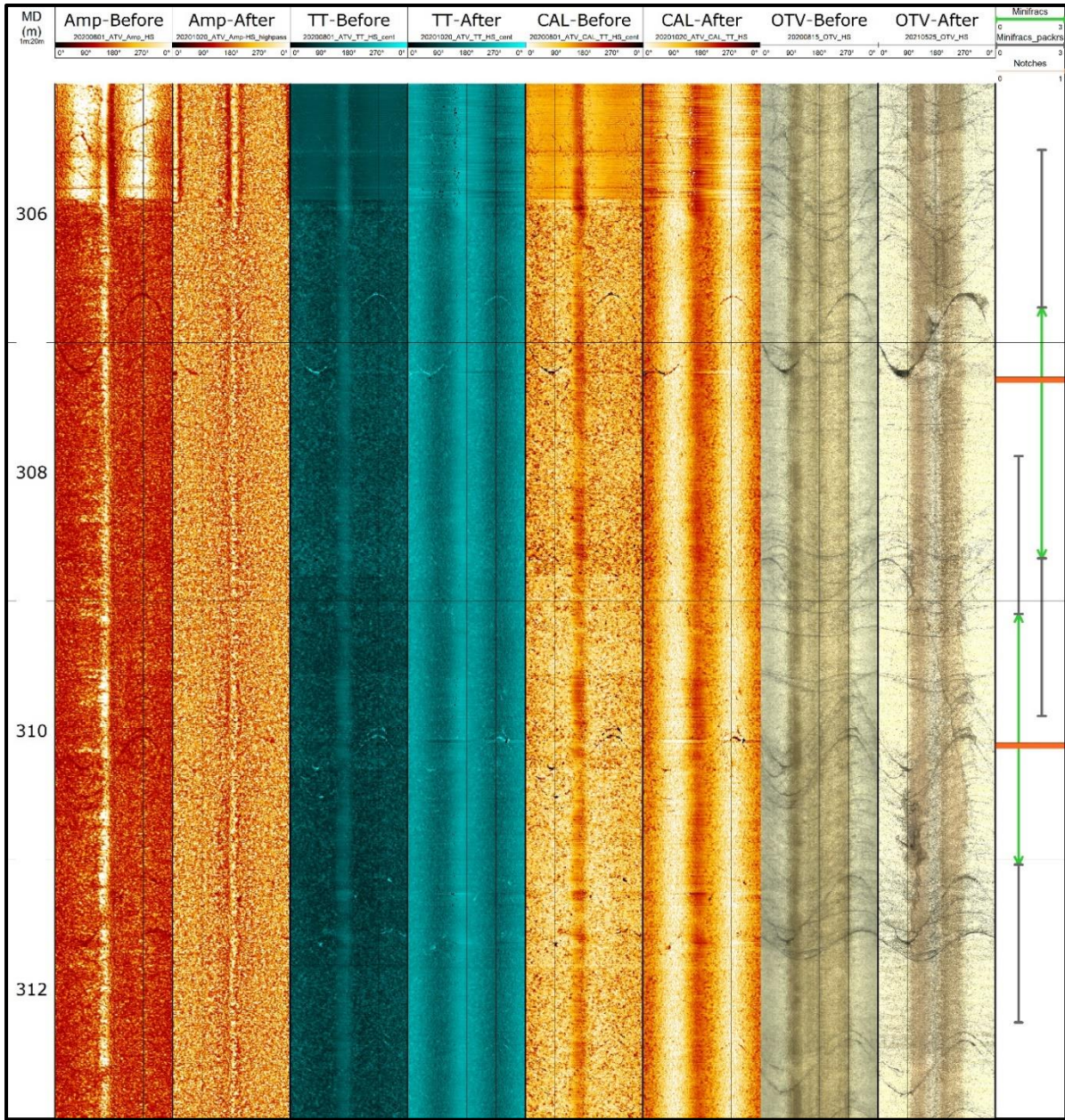
Figure 33. Interval 301.3-303.3m



356

357

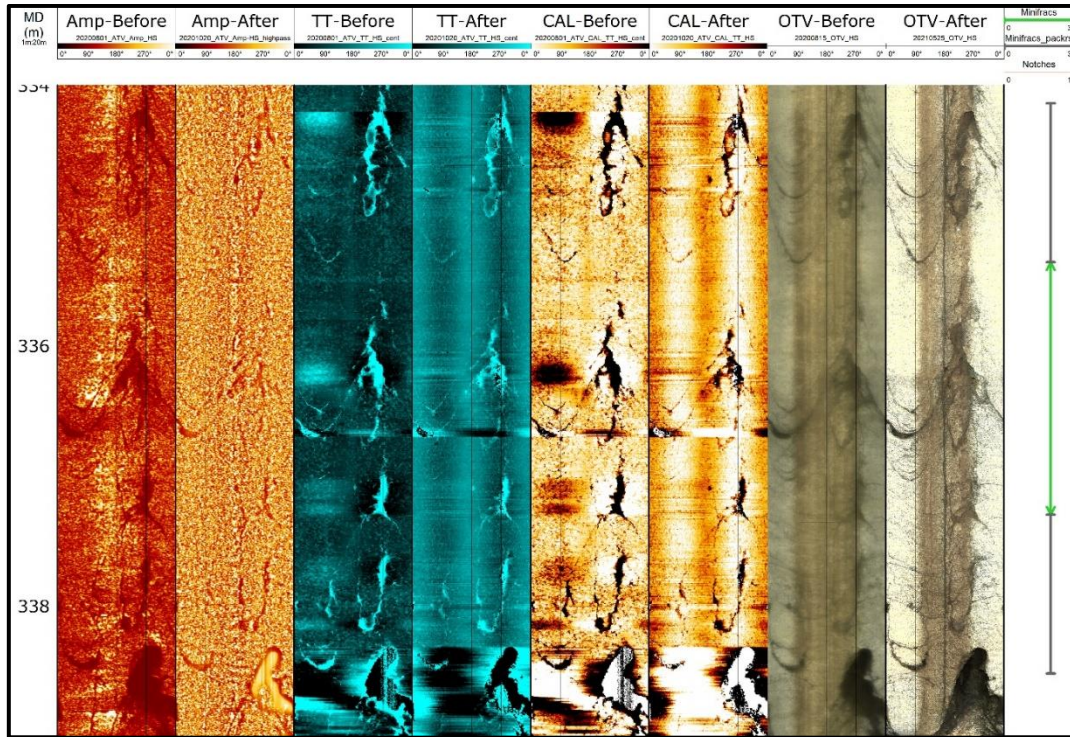
Figure 34. Interval 314.8-316.8m



358

359

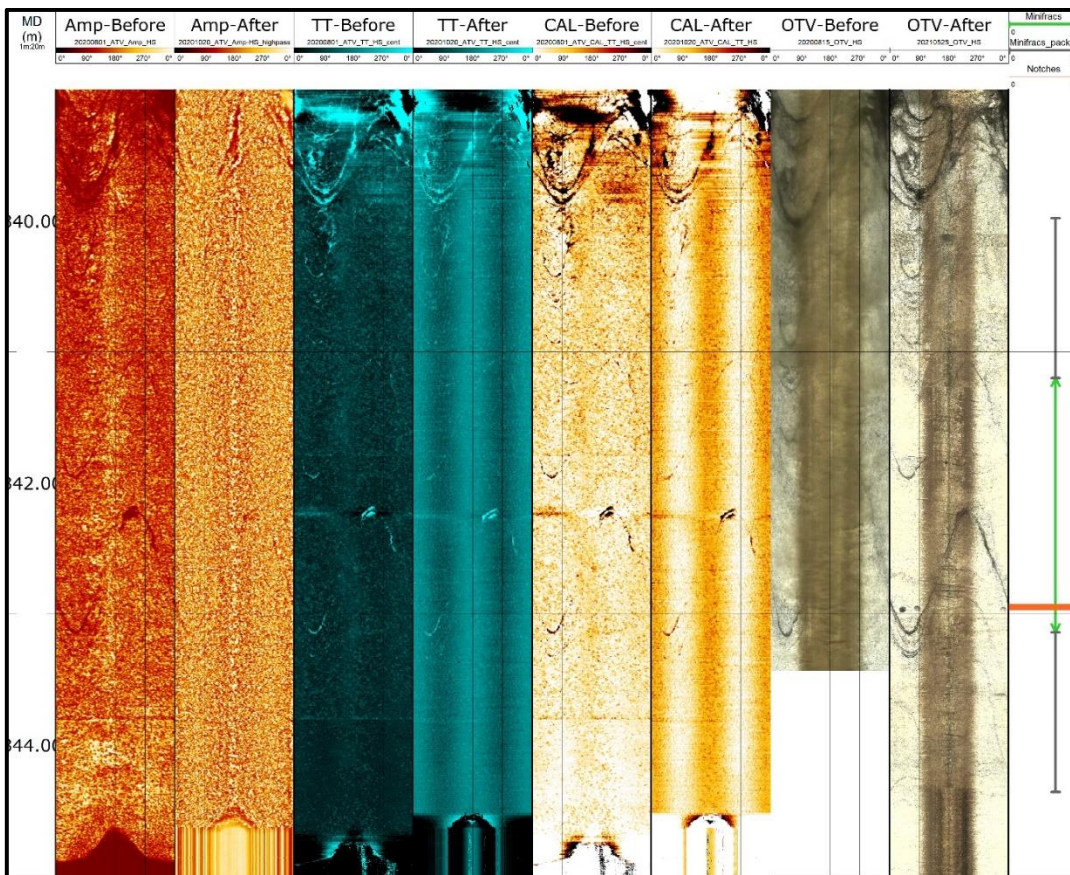
Figure 35. Intervals 306.7-308.7m and 309.1-311.1m



360

361

Figure 36. Interval 335.3-337.3m



362

363

Figure 37. Interval 341.1-343.1m

364 8. Stimulations

365 Three stimulation campaigns were carried out in ST2 in the framework of ZoDrEx. (Table 3).

366 The first set of stimulations was carried out in November 2020 in open hole conditions and with a
367 double packer system. The stimulated intervals are located between 305m and 340m. A second
368 stimulation campaign in May 2021 was carried out also in open hole conditions but this time with a
369 single packer to isolate the bottom of the borehole between 332m and 350m.

370 The third stimulation campaign took place in October 2021 in the cemented and cased borehole and
371 through perforations done between July and October 2021 (see section 6.4). The intervals
372 stimulated during this last campaign are located between depths 275m and 325m.

373

Table 3 Summary of stimulation campaigns

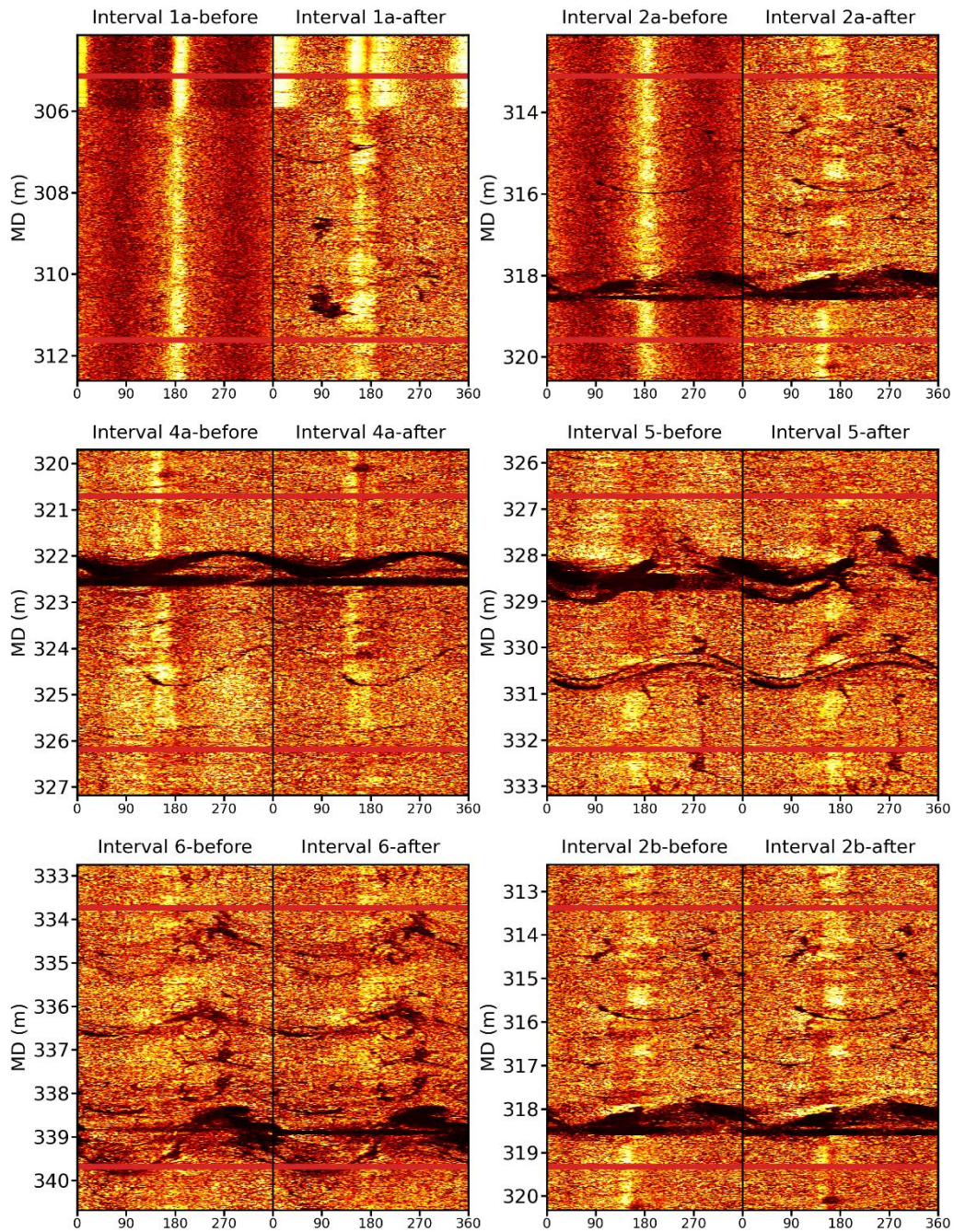
Stimulation Campaign	interval id	Packers					Interval			Datetime	
		Upper		Lower		length	top	base	length	start	end
		top	base	top	base						
Nov2020	1a	303.63	305.13	311.61	313.11	1.5	305.13	311.61	6.48	10/11/2020 19:25:06.0	15/11/2020 21:38:00.0
	2a	311.6	313.1	319.58	321.08	1.5	313.1	319.58		16/11/2020 13:38:54.0	19/11/2020 00:29:00.0
	4a	319.2	320.7	326.18	327.68	1.5	320.7	326.18	5.48	21/11/2020 09:01:10.0	23/11/2020 11:58:43.0
	5	325.22	326.72	332.2	333.7	1.5	326.72	332.2		23/11/2020 20:33:59.0	25/11/2020 21:37:55.0
	6	332.52	333.74	339.68	340.9	1.22	333.74	339.68	5.94	27/11/2020 18:06:42.0	29/11/2020 12:45:38.0
	2b	312.16	313.38	319.32	320.54	1.22	313.38	319.32		29/11/2020 13:34:43.0	29/11/2020 23:14:54.0
	4b	319.4	320.62	326.56	327.78	1.22	320.62	326.56		30/11/2020 00:31:43.0	30/11/2020 12:40:55.0
	1b	304.8	306.02	311.96	313.18	1.22	306.02	311.96		30/11/2020 13:22:13.0	30/11/2020 23:20:40.0
May2021	6sp	331.02	332.52			1.5	332.52	350	12.48	21/05/2021 17:32:00.0	23/05/2021 13:48:00.0
Oct2021	1						305.16	309.29	4.13	06/10/2021 11:20:30.0	08/10/2021 12:06:00.0
	8						281.9	286.03		08/10/2021 13:54:43.0	12/10/2021 17:56:00.0
	7						273.2	277.33		12/10/2021 19:21:00.0	13/10/2021 11:15:00.0
	4						322.15	326.28		13/10/2021 13:33:00.0	14/10/2021 08:40:00.0
	1						305.16	309.29		14/10/2021 10:01:36.0	14/10/2021 12:55:00.0
	4						322.15	326.28		14/10/2021 14:02:00.0	14/10/2021 15:00:00.0
	8						281.9	286.03		14/10/2021 16:27:30.0	15/10/2021 07:13:00.0

376 8.1 November 2020

377 8.1.1 Intervals

378 Five intervals were stimulated during the November 2020 campaign (i.e. 1, 2, 4, 5 and 6). Three of
379 these intervals were re-stimulated during the same campaign (1, 2 and 4). Figure 38 and Figure 39
380 show the before-vs.-after amplitude values from the ATV images for each interval.

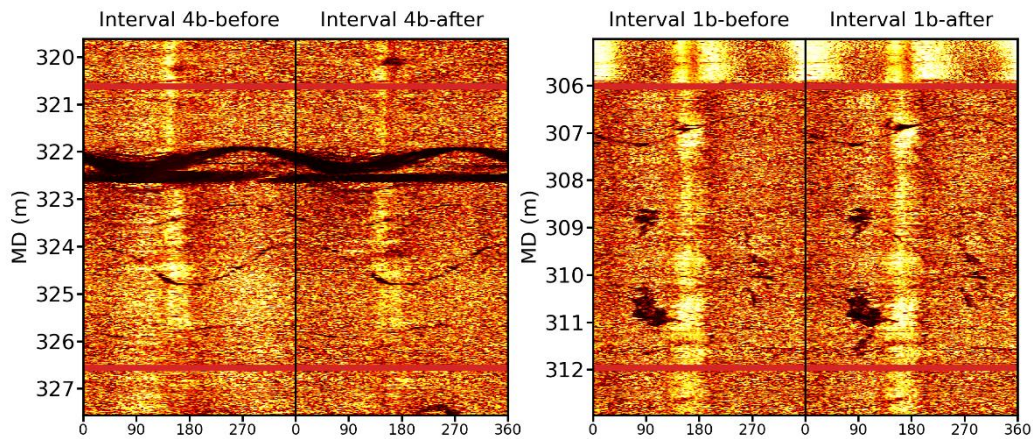
381 Differences between the before and after versions of the ATV are observed in the intervals 1a and 2a
382 where some natural, pre-existing fractures are more visible in the after version of the log. New
383 breakout-like features also appear in the after images of the 1a interval with some further
384 differences after the re-stimulation as it can be seen in the after version of the 1b interval. The
385 effects of the stimulation, observed in intervals 1, 2 and 5 are described and analyzed further in
386 detail in the subchapter "8.1.4. Shear displacement on pre-existing fractures"



387

388

Figure 38. Before vs. After ATV amplitude logs of intervals stimulated in November 2020.



389

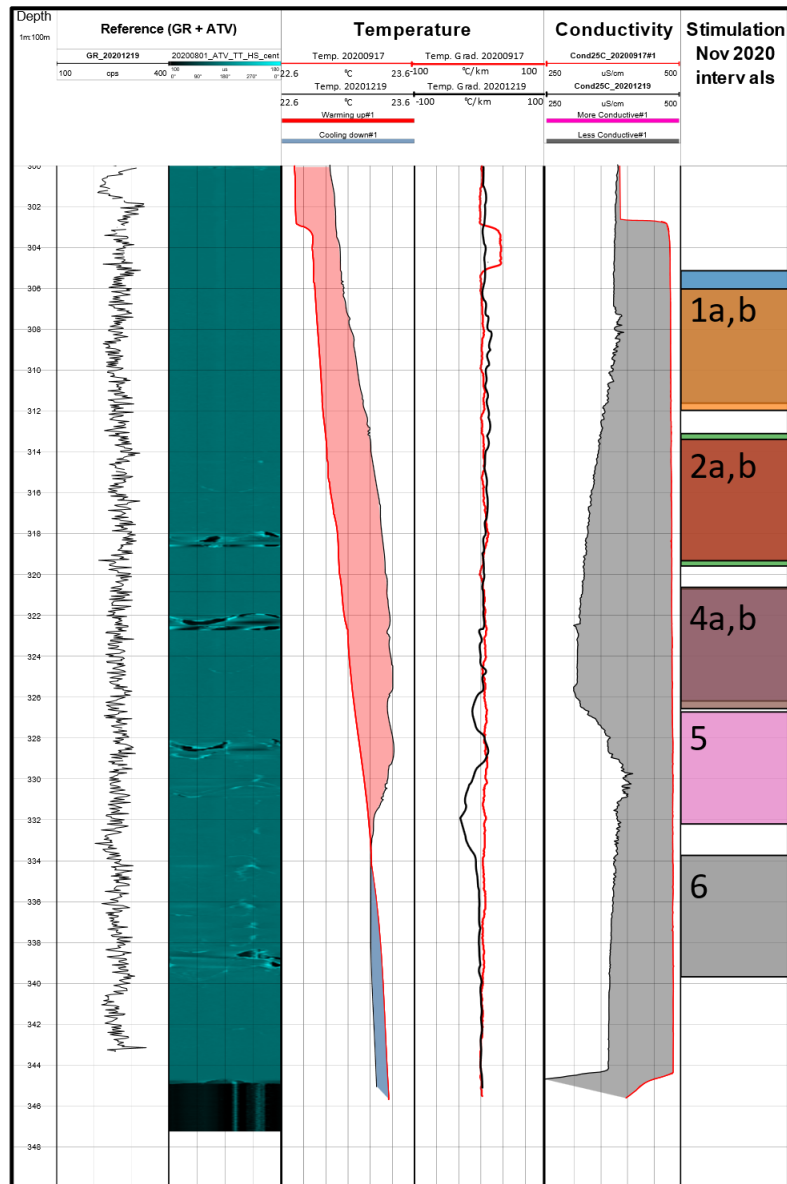
390 *Figure 39. Continuation from Figure 38. Before vs. After ATV amplitude logs of intervals stimulated in*
 391 *November 2020.*

392 **8.1.2 Fluid Temperature & Conductivity**

393 Two FTC logs are compared in Figure 40, corresponding to runs before the stimulation (September
 394 17th), and after the end of the stimulation (December 19th).

395 The fluid temperature increased above 334m while it decreased below. The temperature gradient
 396 remains largely unchanged except for the disappearance of the temperature anomaly at 303m and
 397 the appearance of new ones between 326m-334m. The significant cooling of the water column
 398 below 329m is probably due to the backflow of injected water from interval 6 after the end of the
 399 stimulation.

400 The correspondent conductivity anomaly at 303m was also smoothed out after the stimulation. In
 401 general, conductivity decreased in the whole interval with important changes in the trend at 308m,
 402 326m and 330m. Conductivity values below 330m are equivalent to those above 308m. This shows
 403 the salinity decrease only affected the one between intervals 1 and 5 when the December 19th log
 404 was run.



405

406

Figure 40. Fluid temperature and conductivity before and after the November 2020 stimulation.

407

8.1.3 Newly formed Breakouts

408

New breakouts are observed in ATV logs between 300-315m MD after the November 2020

409

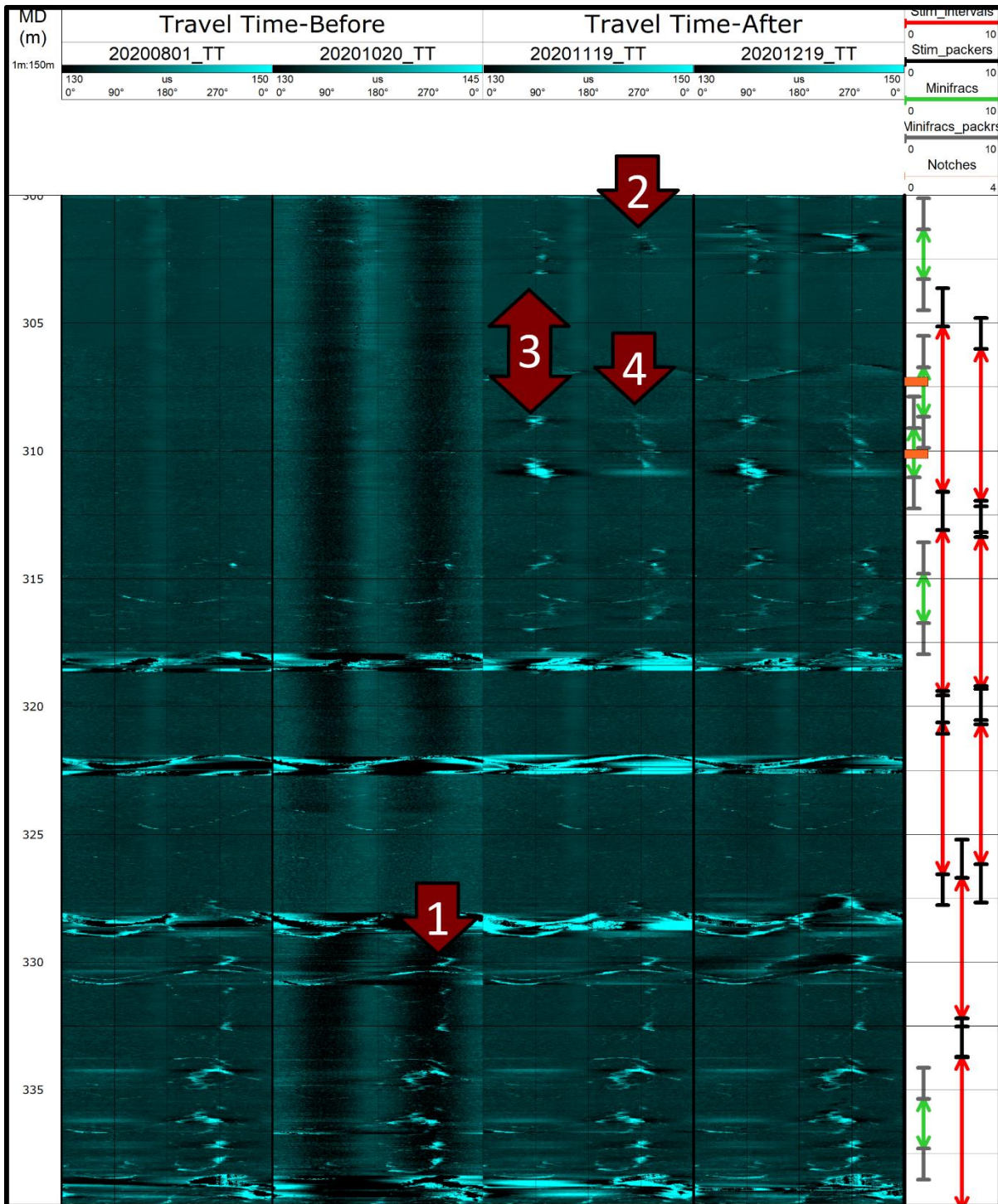
stimulation campaign. It is not entirely clear if these breakouts formed as a consequence of the

410

stimulation treatments or by wearing of the borehole due to the rubbing of logging tools and packer

411

systems.

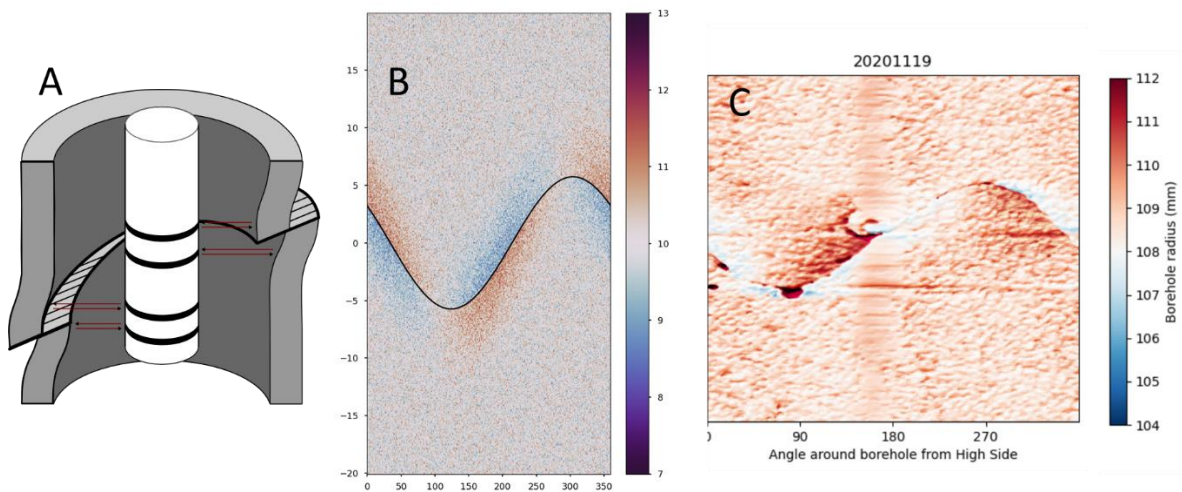


412

413 *Figure 41. Four different ATV logs, two pre-stimulation (August and October 2020), one during*
 414 *stimulation (November 2020) and one post stimulation (December 2020). Pre-existing breakouts (1)*
 415 *vs. new breakouts created during the stimulation carried out in November 2020 (2-4). New BOs*
 416 *concentrate in the upper stimulated intervals. At this scale of observation, new BOs are not*
 417 *necessarily located near the biggest natural fractures. Instead, they seem to locate around smaller*
 418 *fractures reactivated by the stimulation.*

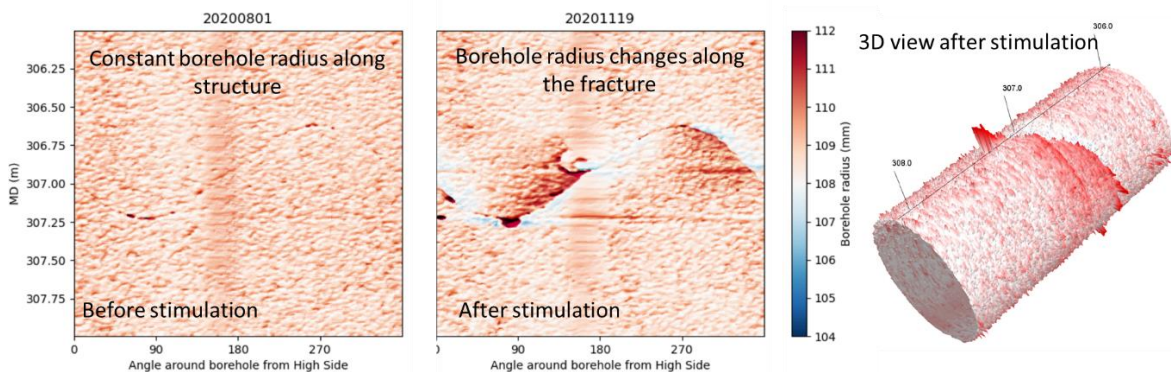
419 8.1.4 Shear displacement on pre-existing fractures

420 The travel time of the acoustic signal, measured during the ATV acquisition, allows the 3D
 421 reconstruction of the borehole wall surface. This estimated 3D "caliper" was used here to identify
 422 and analyze the potential changes in the borehole wall induced by the shear stimulation campaigns
 423 of October 2020 and May 2021. A shear displacement along a structure intersecting the borehole
 424 (Figure 42A) will reduce and increase the distance between the borehole wall and the borehole axis
 425 in different places along the fracture as shown by the synthetic 3D caliper in Figure 42B. Figure 42C
 426 shows a real natural fracture in ST2 where the same pattern of cyclic caliper variation along the
 427 fracture can be observed.



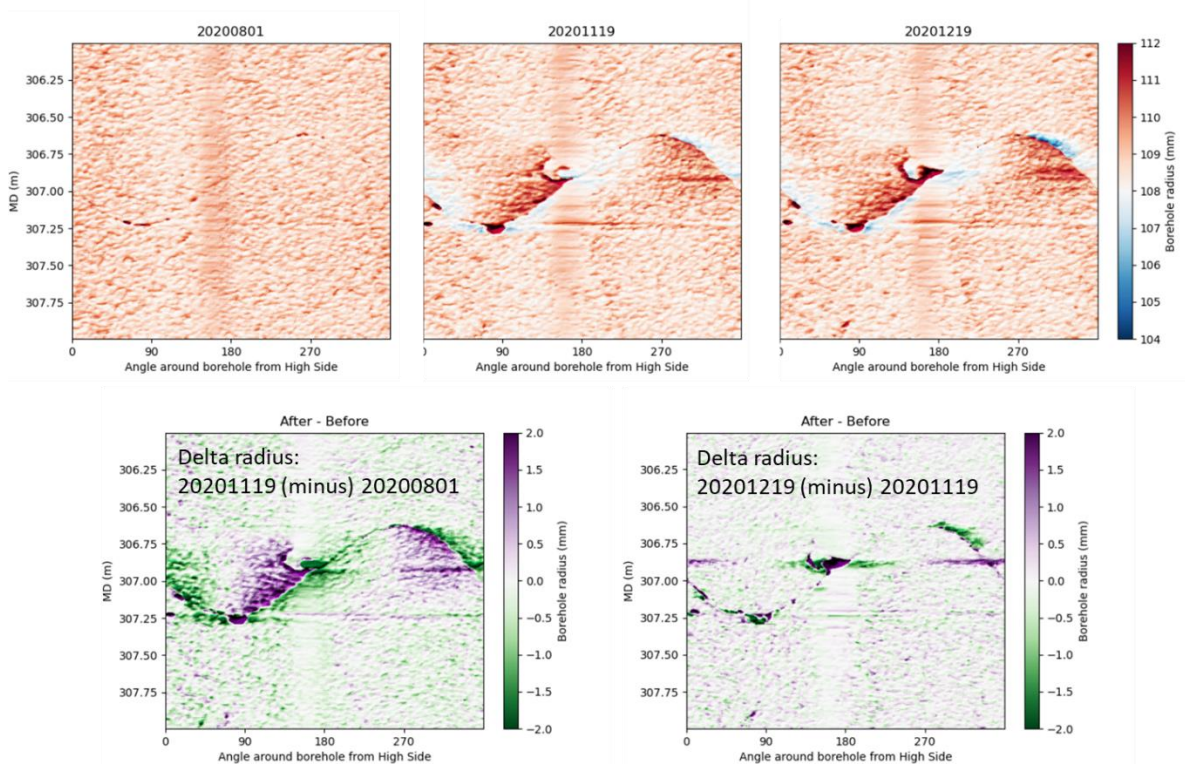
428
 429 *Figure 42 A) Sketch showing how a constant shear displacement vector applied on a fracture affect*
 430 *the distance between the borehole wall and the borehole axis. B) Synthetic simulated case with a*
 431 *fracture and an arbitrary shear displacement vector. Blue zones (decreased distance) intercalate with*
 432 *red zones (increased distance) along the fracture. C) A real case from ST2s showing a similar pattern*
 433 *as in B.*

434 The comparison of ATV logs from before and after the stimulation allowed us to confirm that the
 435 observed effect was caused by the shear stimulation (Figure 43).



436
 437 *Figure 43. Example of sheared structure after stimulation. This structure can be found in interval 1a*
 438 *and 1b in Figure 38.*

439 The amplitude of the shear displacement was the biggest after the 1st stimulation as shown in Figure
 440 44. The re-stimulation carried out shortly afterwards didn't bring much of a change in the shear
 441 displacement.

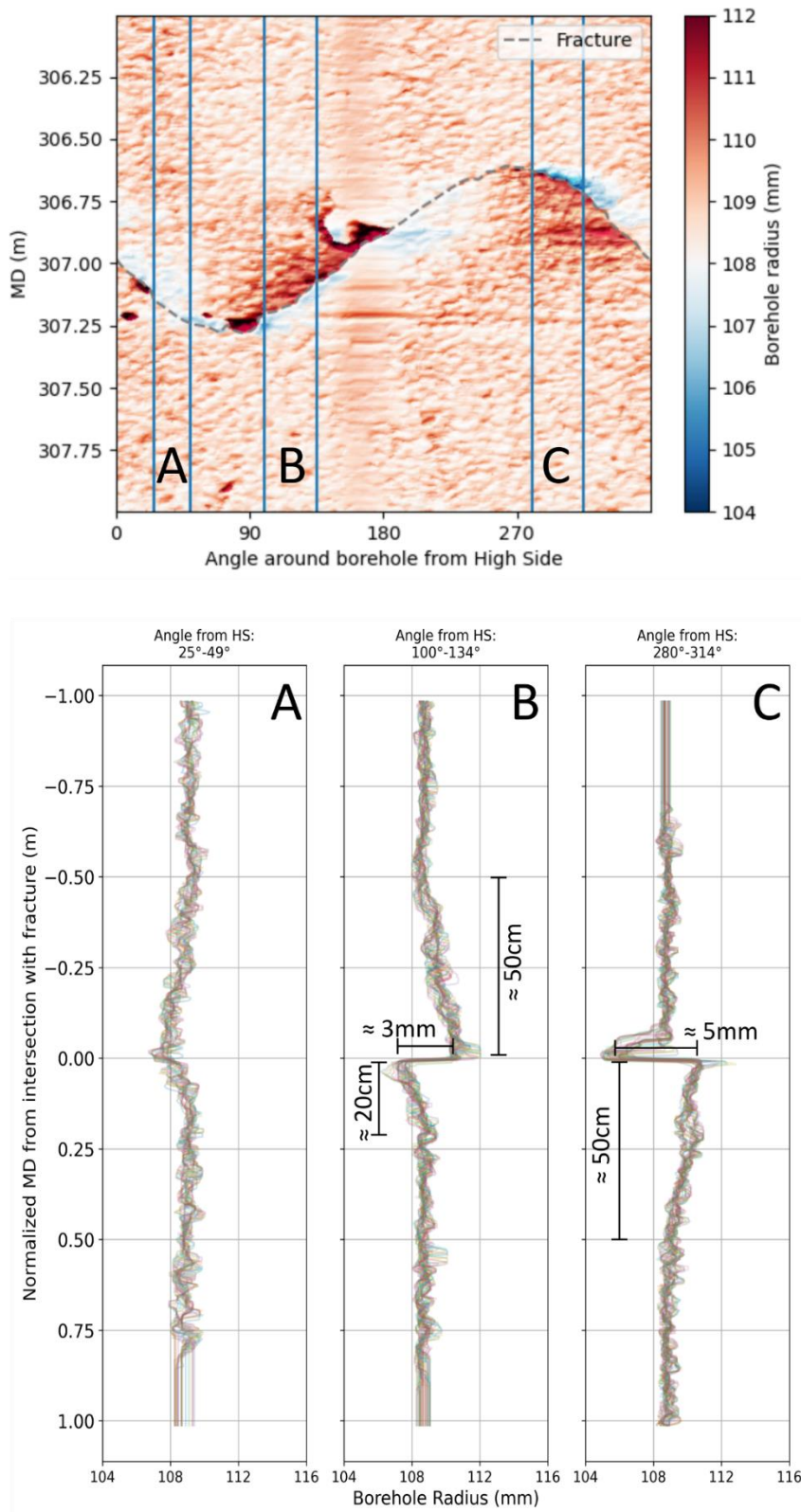


442
 443 *Figure 44. Sequential development of the deformation. Most displacement takes place in the 1st*
 444 *stimulation.*

445 The identified displacement can be directly measured in the 3D caliper log at different places along
 446 the fracture (Figure 45). Maximum displacements of 5 mm could be measured. The zone affected by
 447 this deformation can extend up to 50cm away from the fracture.

448 The above-described shear displacement was identified in 3 different structures along ST2 in
 449 intervals 1, 2 and 5 (Figure 46). In each case, displacements between 1-5 mm were measured. The
 450 respective displacement vectors indicate that the shear sense was normal. This is at odds with the
 451 theoretical reverse displacement vector predicted when applying the stress state for the BULGG
 452 assessed in short boreholes in the vicinity of the tunnel (Ma et al., 2019) (Figure 47).

453 The three fractures with shear displacement share the common characteristic of being relatively
 454 simple structures that express as thin, linear features in the image logs. The lack of observed shear
 455 displacement in other intervals does not mean that it didn't take place, but rather that other
 456 structures are too complex, and the borehole wall is too perturbed by the drilling around these more
 457 complex fractures.

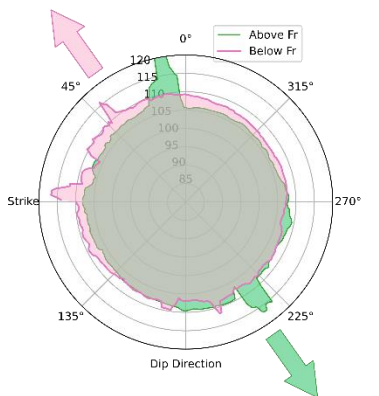
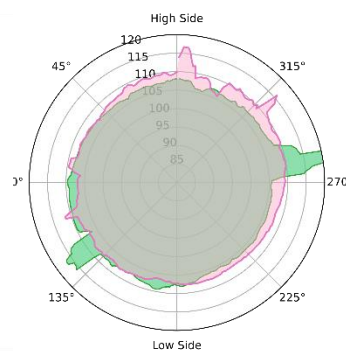
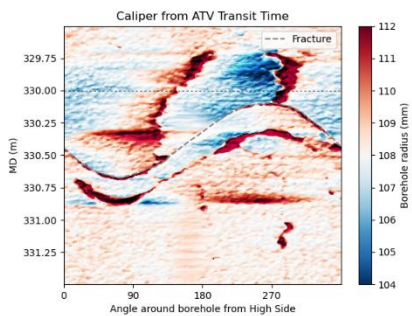
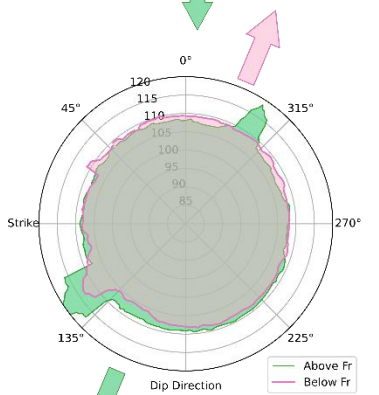
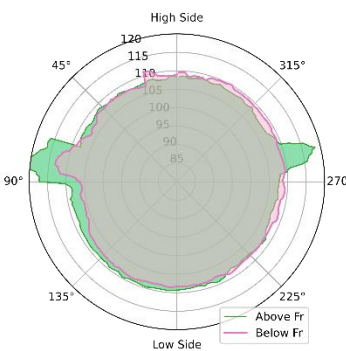
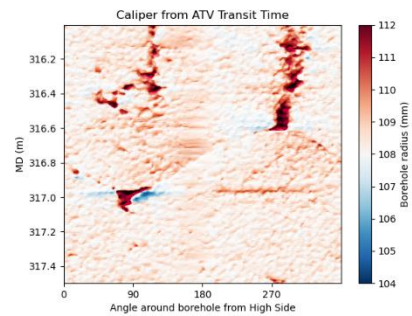
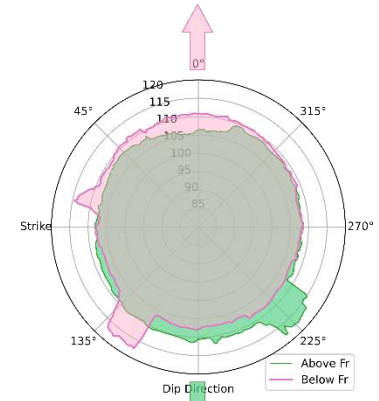
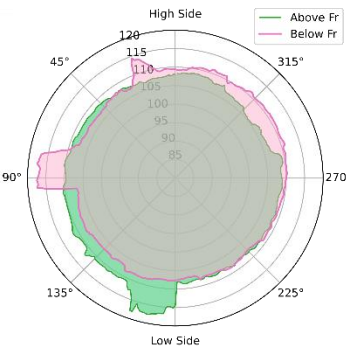
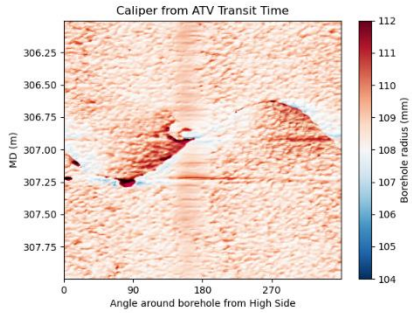


458

459 *Figure 45. 3D caliper profiles across a fracture reactivated during the stimulation. Displacements of*
 460 *up to 5mm could be detected on acoustic logs. The effects of displacement can be seen as far as*
 461 *50cm away from the fracture.*

Borehole Framework

Fracture Framework

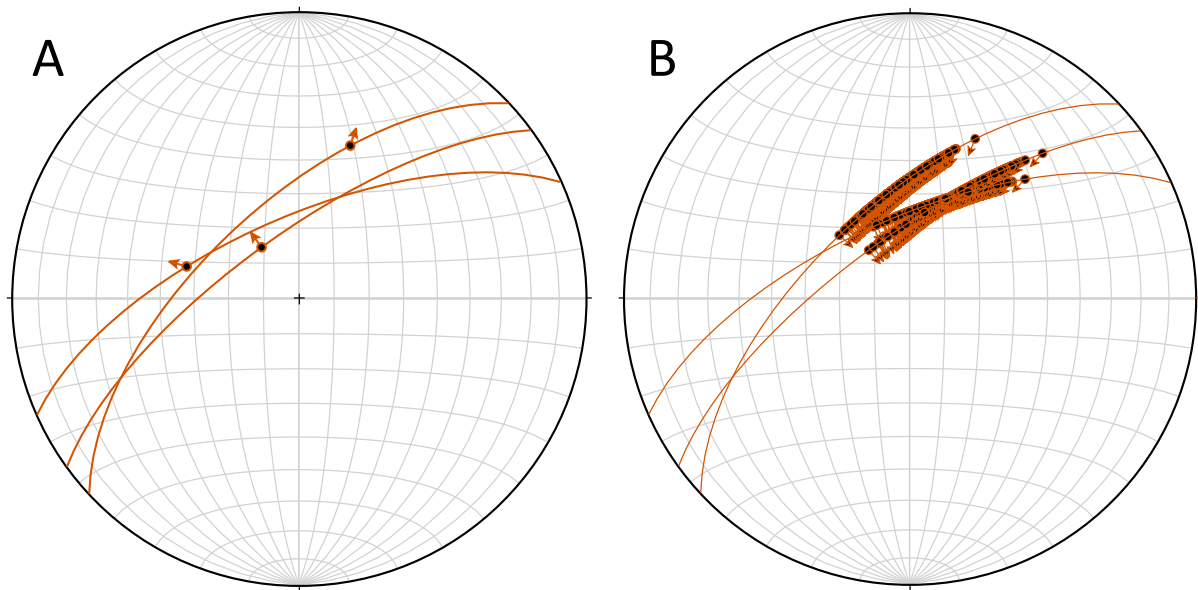


462

463

464

Figure 46. Three structures showing shear displacement after stimulation. In all cases the compartment above the fracture subsided. Each fracture is located in 3 different intervals (1, 2 and 5)



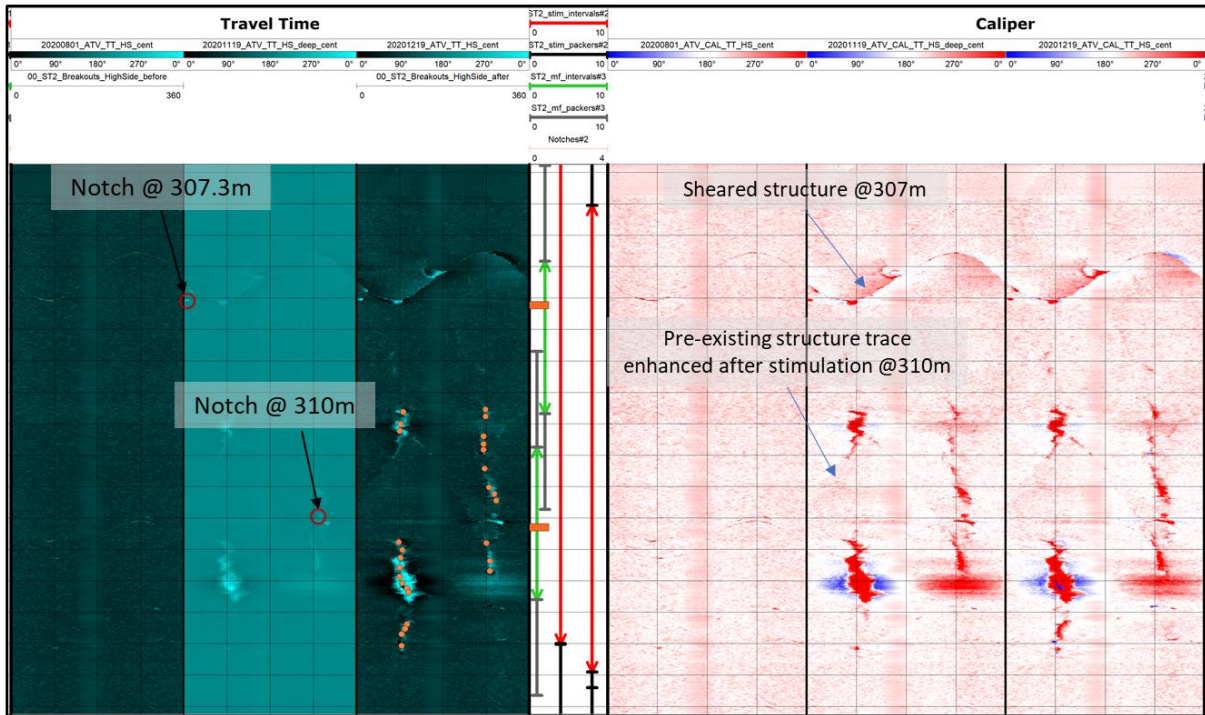
465

466 *Figure 47. Stereonet showing the 3 fracture planes where shear displacement was identified in ST2.*

467 *A) The measured directions of the respective displacement vectors, B) Theoretical displacement*
 468 *vectors with the stress state from Ma et al. (2019).*

469 **8.1.5 Influence of notching on stimulation results**

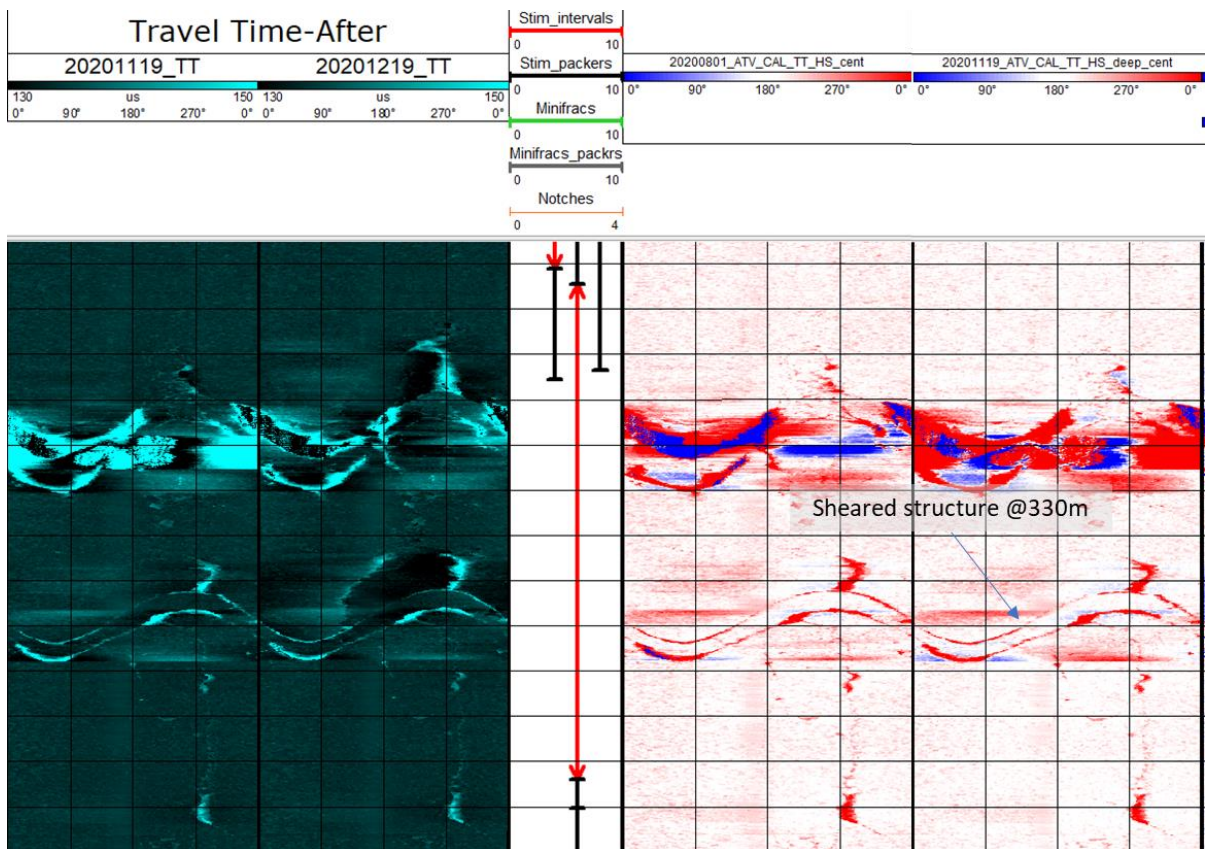
470 Interval 1 had been perforated in October 2020 with 2 notches prior to the stimulation. These
 471 notches are clearly observed in ATV logs at 307.3m and 310m (Figure 21). A third notch was done at
 472 275.6m but no stimulation was performed at this depth. It is difficult to assess whether these
 473 notches had an influence in the outcome of the stimulation. On one hand, the notch at 307.3 m is
 474 adjacent to the fracture where a shear displacement was measured after the stimulation (see 8.1.4
 475 Shear displacement on pre-existing fractures), but on the other hand 2 other fractures with shear
 476 displacement lacked of any perforation nearby prior to the stimulation.



477

478

Figure 48. Sheared structures at 307m and 310m MD coincide with notching locations.



479

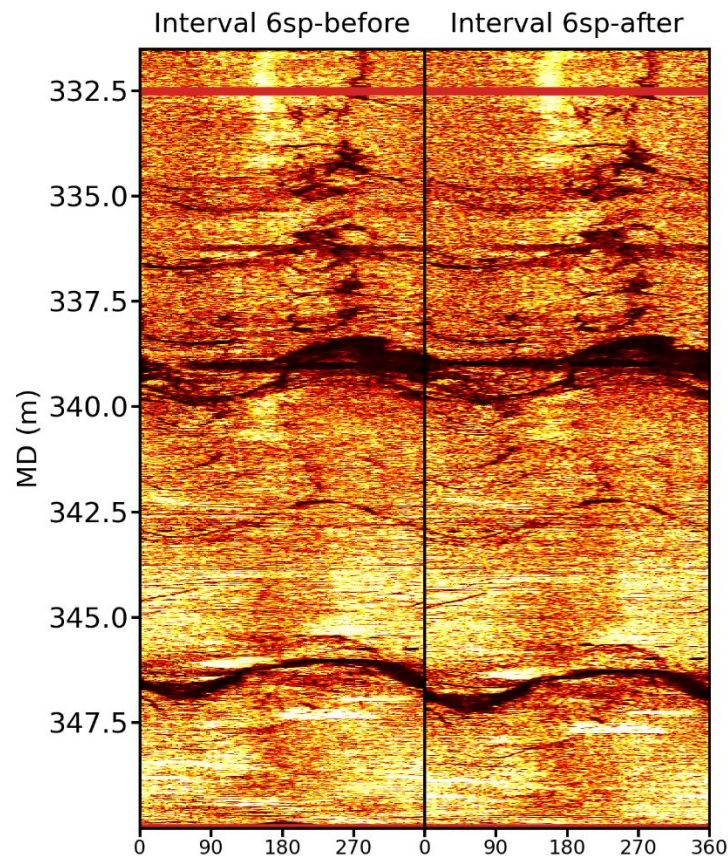
480

Figure 49. Sheared structures at 330m MD is not associated to any notching location.

481 8.2 May 2021

482 8.2.1 Intervals

483 In May 2021 the bottom of the borehole was stimulated by isolating the section below 332.5m.
 484 Figure 50 shows the before-vs-after ATV log of this interval. No clear evidence of changes can be
 485 observed in the ATV log.



486

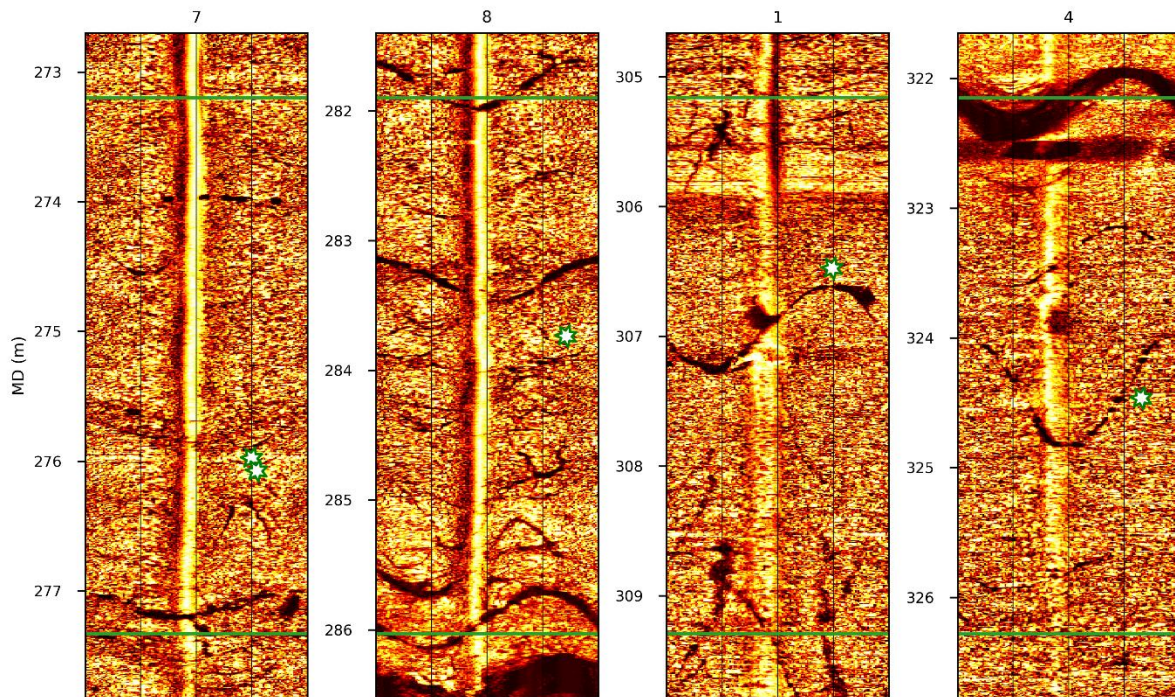
487

Figure 50. Interval stimulated in May 2021.

488 8.3 October 2021

489 8.3.1 Intervals

490 The last stimulation campaign carried out in ST2 took place in October 2021 after the borehole was
 491 cased & cemented and perforations were done at different depths. Logs were not run after this set
 492 of stimulations because no effect is expected to be seen in the cemented borehole wall. Figure 51
 493 show the ATV logs for each stimulated interval and the places where notching was performed prior
 494 to the stimulation.



495
496
497

Figure 51. Intervals stimulated during the October 2021 campaign. Green stars mark the places where notches were perforated in the casing.

498 9. References

- 499 Zhang, S., K. Broeker, R. van Limbor, X. Ma, in press, In situ stress variations around reservoir-scale
500 fault zones.
- 501 Ma, X., N. G. Doonechaly, M. Hertrich, V. Gischig, G. Klee, 2019, Preliminary in situ stress and
502 fracture characterization in the Bedretto Underground Laboratory, Swiss Alps: implications on
503 hydraulic stimulation, 14th International Congress on Rock Mechanics and Rock Engineering (ISRM
504 2019), Foz do Iguassu, Brazil, September 13-18, 2019.

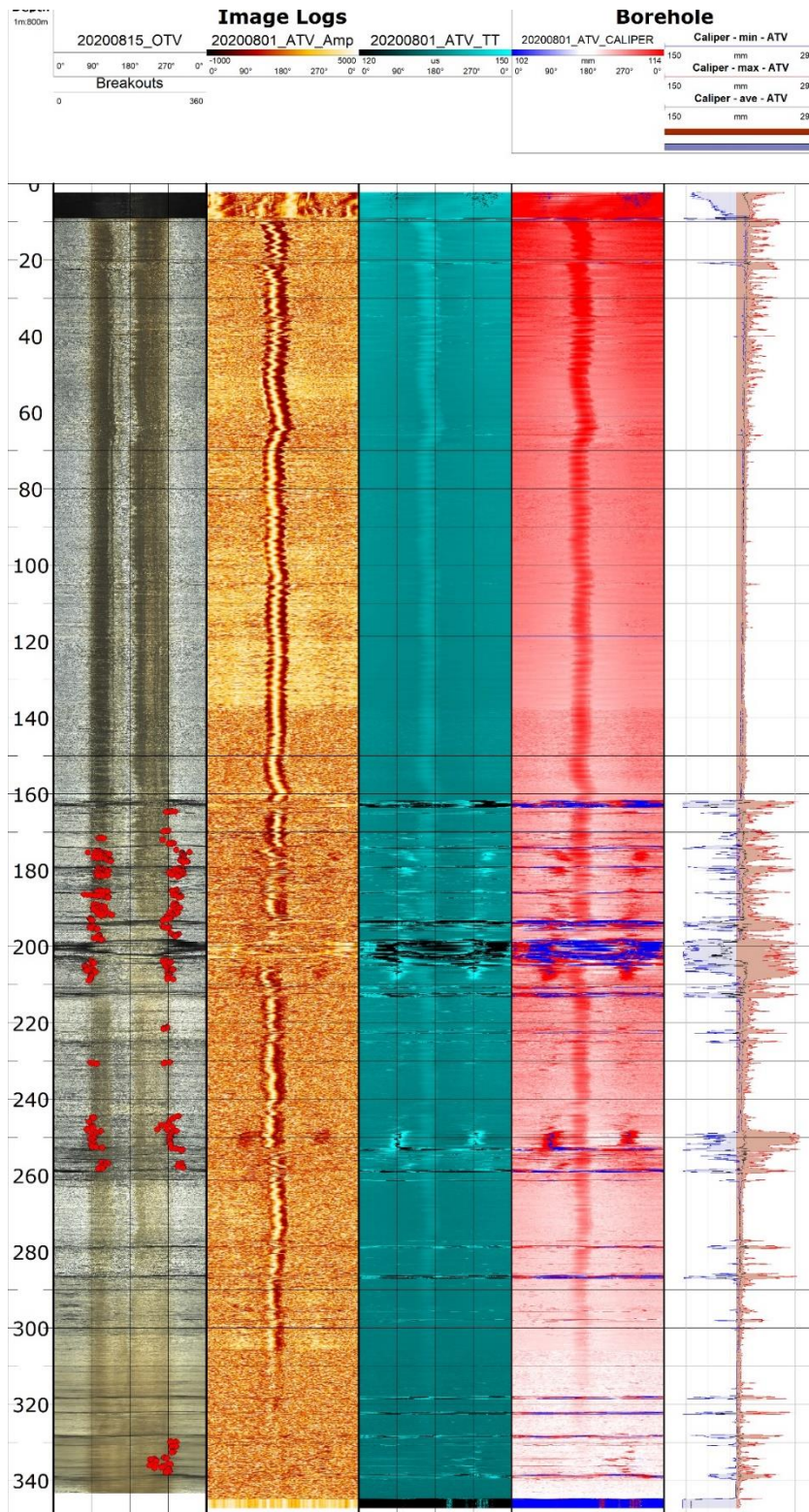
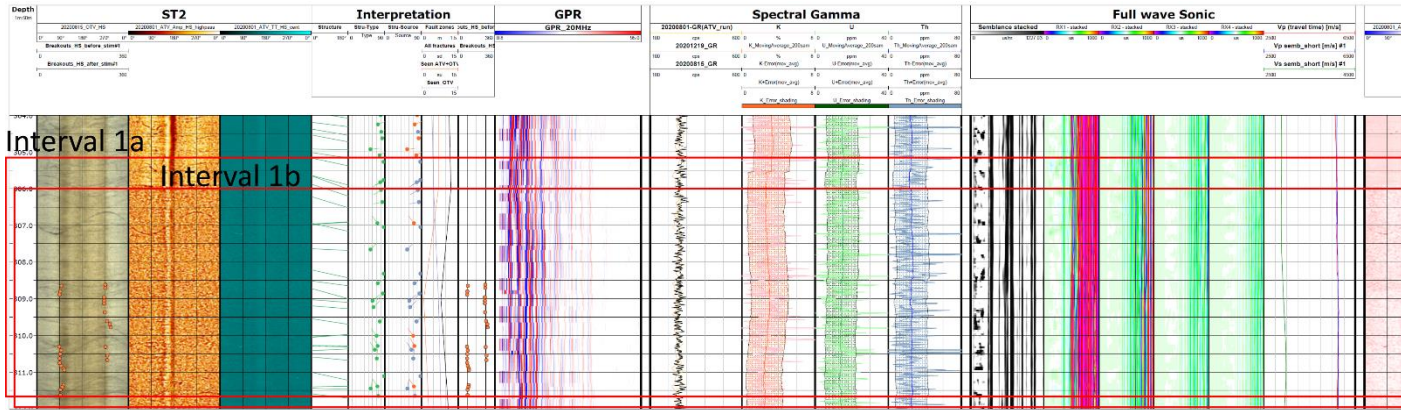


Figure 52. Image logs (OTV & ATV), breakouts (red points) and caliper calculated from acoustic travel time in ST2 after drilling. Breakouts and washouts form inside intervals of strong deformation (presence of fault zones and increased fracture frequency). Sections with small amounts or no brittle fractures do not develop breakouts.

508

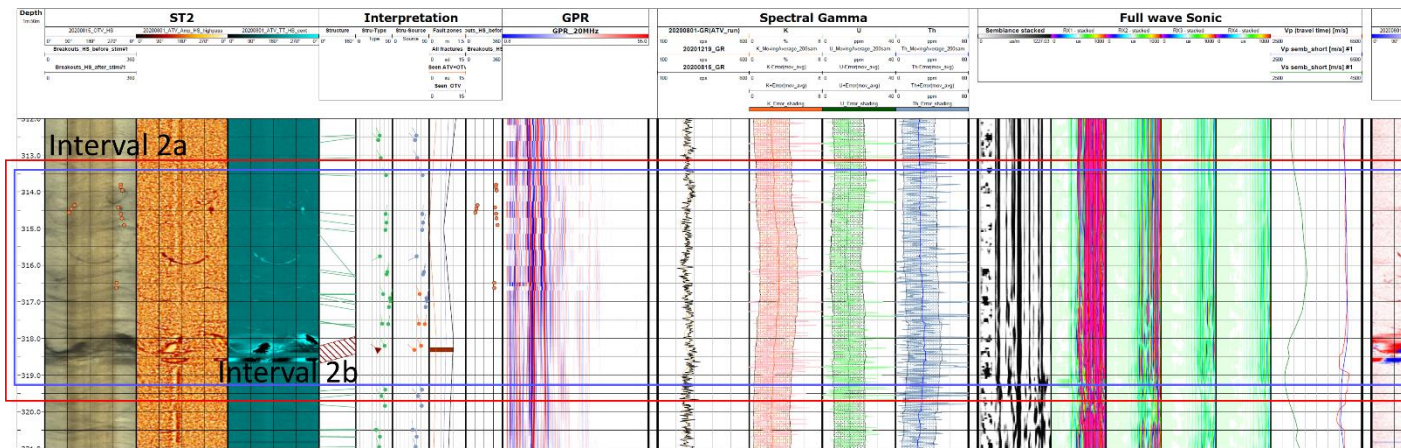
509 10.1 Stimulation November 2020 – Full borehole logs

510



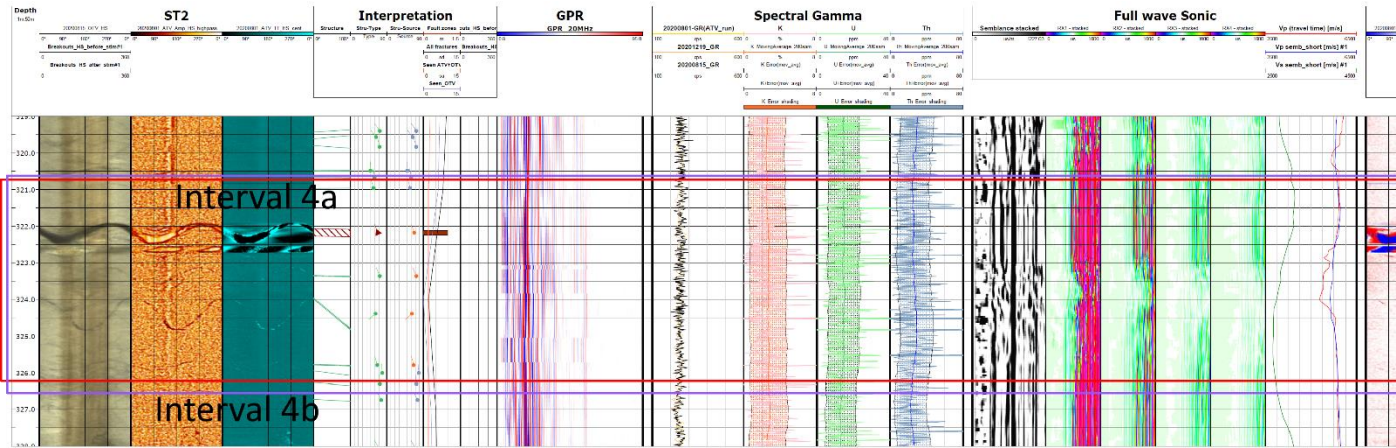
511

512 *Figure 53. Stimulation-November 2020. Intervals 1a and 1b.*



513

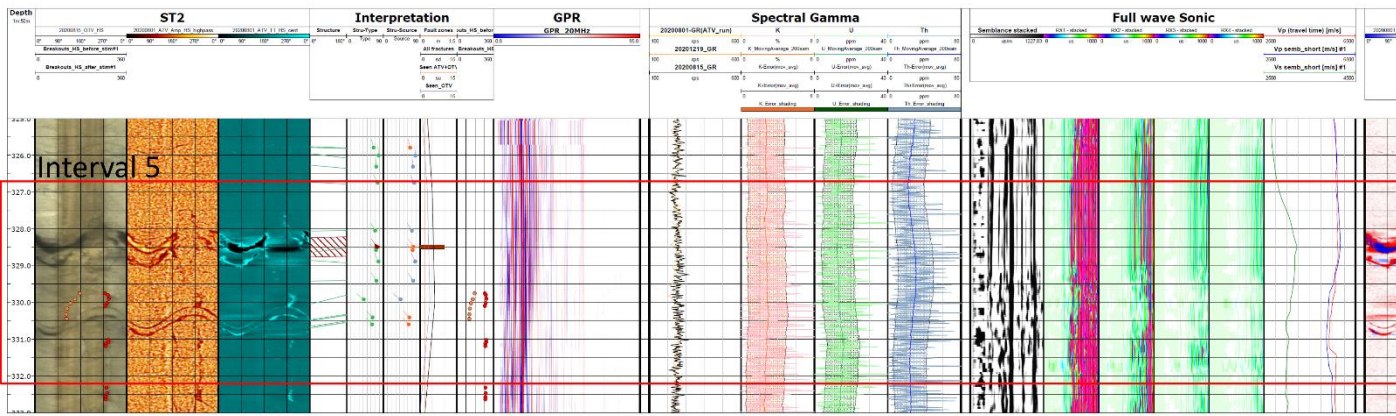
514 *Figure 54. Stimulation-November 2020. Intervals 2a and 2b.*



515

516

Figure 55. Stimulation-November 2020. Intervals 4a and 4b.



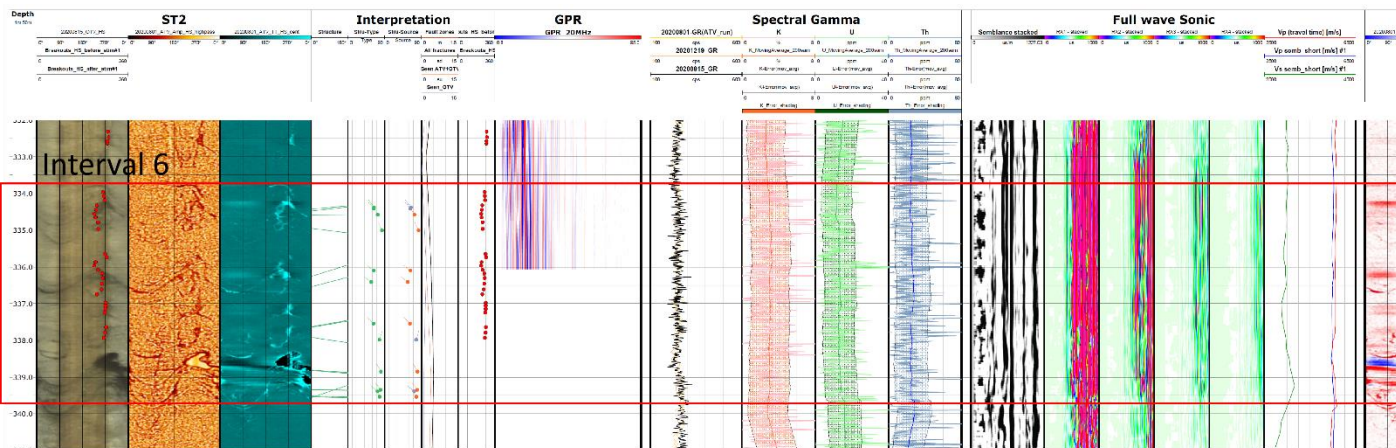
517

518

Figure 56. Stimulation-November 2020. Interval 5.

519

520



521

522

Figure 57. Stimulation-November 2020. Interval 6.

